3 1176 00081 9442

NATIONAL ADVISORY COMMITTEE FOR AERONAUTICS

TECHNICAL NOTE

No. 1046

PRELIMINARY WIND-TUNNEL INVESTIGATION AT LOW SPEED OF STABILITY AND CONTROL CHARACTERISTICS OF SWEPT-BACK WINGS

By William Letko and Alex Goodman

Langley Memorial Aeronautical Laboratory
Langley Field, Va.

FOR REFERENCE

NOT TO BE TAKEN FROM THIS ROOM

Washington
April 1946

NACA LIBRARY
LANGLEY MEMORIAL AERONAUTICAL
LABORATORY

NATIONAL ADVISORY COMMITTEE FOR AERONAUTICS

TECHNICAL NOTE NO. 1046

PRELIMINARY WIND-TUNNEL INVESTIGATION AT LOW SPEED OF STABILITY AND CONTROL CHARACTERISTICS OF SWEPT-BACK WINGS

By William Letko and Alex Goodman

SUMMARY

Tests were conducted on untapered constant-span wings of 0°, 30°, 45°, and 60° sweepback. The purpose of these tests was to investigate the effect of sweepback on stability and control characteristics.

The data showed large changes in longitudinal stability at moderate lift coefficients for the 45° and 60° swept-back wings. The lateral stability, the slope of the lift curve, and the effectiveness of the aileron and the split flap at small angles of attack varied with angle of sweepback about as much as would be expected from simple theoretical considerations. Spoilers were much less effective than would be indicated by simple theory.

All the swept wings with flaps neutral reached a maximum value of about 20° effective dihedral at some lift coefficient. Drooping the wing tips decreased the slope of rolling-moment curve plotted against angle of yaw. Because the reduction increased with increase in lift coefficient, drooping the tips appeared to be a promising means of reducing the unfavorable lateral stability characteristics of wings with large sweepback.

The ailerons were capable of trimming out the rolling moment caused by only small angles of sideslip for the highly swept-back wings. The small change in pitching moment caused by aileron deflection indicated that wing-tip elevators having swept-back hinge lines would be relatively ineffective on highly swept-back wings.

The maximum lift with flaps neutral remained about the same for all angles of sweepback. The increment of

maximum lift caused by the split-flap deflection decreased with angle of sweepback to approximately 0 for the 60° swept-back wing.

INTRODUCTION

Much interest has been shown in the possibility of using wings with large amounts of sweepback for high-speed missiles and aircraft. Analyses presented in references 1 and 2 show that the lift on a swept-back wing depends primarily on the component of velocity normal to the wing leading edge. Reference 3 shows that this component of velocity also is a most important factor in determining compressibility effects and points out that, from consideration of compressibility, the critical flight Mach number of a swept-back wing should be higher than that of an unswept wing. In order to minimize the adverse effects of compressibility at high Mach numbers, the angle of sweep should be such that the component of velocity normal to the leading edge does not exceed that corresponding to the critical Mach number of the airfoil sections.

Since very little data are available on wings having angles of sweep greater than 30°, tests of an exploratory nature were made of wings having angles of sweepback of 0°, 30°, 45°, and 60°. These tests were made in the 6- by 6-foot test section of the Langley stability tunnel to investigate at low speeds the stability and control characteristics of swept-back wings. The effect of sweepback on the effectiveness of an aileron, a split flap, and a spoiler was investigated for each sweepback angle tested. The effect of a drooped tip was investigated for the 45° swept-back wing, and the effect of increased aspect ratio was investigated for the 0° and 45° swept-back wings.

Although these tests were made at low airspeeds, the data are also of importance in application to transonic speed because, as pointed out in reference 3, if the wings are designed with proper sweep, the wing will have the same characteristics as at subcritical speed.

SYMBOLS

The data are referred to the stability axes, which are a system of axes having their origin at the quarter chord of the mean aerodynamic chord and in which the Z-axis is in the plane of symmetry and perpendicular to the relative wind, the X-axis is in the plane of symmetry and perpendicular to the Z-axis, and the Y-axis is perpendicular to the plane of symmetry. All moments are given about the quarter chord of the mean aerodynamic chord.

C_L	lift coefficient $\left(\frac{L}{qS}\right)$
$C_{L_{max}}$	maximum lift coefficient
C_X	longitudinal-force coefficient $\left(\frac{X}{qS}\right)$
C_Y	lateral-force coefficient $\left(\frac{Y}{qS}\right)$
C_l	rolling-moment coefficient $\left(\frac{L'}{qSb}\right)$
C_m	pitching-moment coefficient $\left(\frac{M}{qS\bar{c}}\right)$
C_n	yawing-moment coefficient $\left(\frac{N}{qSb}\right)$
L	lift
X	longitudinal force
Y	lateral force
L'	rolling moment about X-axis
M	pitching moment about Y-axis
N	yawing moment about Z-axis

q dynamic pressure $\left(\frac{1}{2}\rho V^2\right)$

ρ mass density of air

V free-stream velocity

S wing area

c chord of wing, measured parallel to axis of symmetry

$\bar{c}$ mean geometric chord of wing, measured parallel to axis of symmetry $\left(\frac{2}{S}\int_0^{b/2} c^2\,db\right)$

b span of wing, measured perpendicular to axis of symmetry

$\bar{x}$ distance from leading edge of root chord to the quarter-chord of the mean geometric chord $\left(\frac{2}{3}\int_0^{b/2} cx\,db\right)$

x distance of the quarter-chord point of any chordwise section from the leading edge of root section

C_{L_α} slope of the curve of lift coefficient plotted against angle of attack

C_{l_ψ} slope of the curve of rolling-moment coefficient plotted against angle of yaw

C_{n_ψ} slope of the curve of yawing-moment coefficient plotted against angle of yaw

$C_{l_{\delta_a}}$ slope of the curve of rolling-moment coefficient plotted against aileron angle

α angle of attack, measured in plane of symmetry, degrees

ψ angle of yaw, positive when right wing is back, degrees

Λ angle of sweepback, degrees

δ_a aileron deflection, measured in a plane perpendicular to leading edge, degrees

δ_f flap deflection, measured in a plane perpendicular to leading edge, degrees

A aspect ratio (b^2/S)

E_e effective edge-velocity correction factor for lift (reference 4)

E'_e effective edge-velocity correction factor for rolling moment (reference 4)

η aspect-ratio correction factor for lift

$$\left(\frac{\left(\frac{A}{E_eA + 2}\right)_0}{\left(\frac{A}{E_eA + 2}\right)_{\Lambda=0}}\right)$$

η' aspect-ratio correction factor for rolling moment

$$\left(\frac{\left(\frac{A}{E'_eA + 4}\right)_0}{\left(\frac{A}{E'_eA + 4}\right)_{\Lambda=0}}\right)$$

where subscript 0 refers to unswept wings having the same wing-panel shape as the swept-back wings, and the subscript $\Lambda = 0$ refers to the wing tested with zero sweepback.

APPARATUS AND MODELS

The present tests were conducted in the 6- by 6-foot test section of the Langley stability tunnel.

The model consisted of two rectangular wings of the NACA 23012 airfoil section. The wings were first cut to obtain an angle of 60° sweepback and then were fastened together with steel brackets. The model was cut successively to obtain angles of sweepback of 45°, 30°, and 0°. For all the wings tested the chordwise dimension of the wing measured perpendicular to the leading edge was 10 inches. Most of the tests were made on wings having a span of 50 inches. A few tests of the 0° and 45° swept-back wings were made with spans of 40.92 and 58 inches, respectively, each model having an aspect ratio of 4.13. The aspect ratio of the wings varied with each angle of sweepback. (See fig. 1.)

The right wing of each model was equipped with a plain 0.20c chord aileron, which had a span equal to one-half the semispan of the wing. With a change in angle of sweepback the aileron and wing were cut in such a way that the span of the aileron remained equal to one-half the semispan of the wing. The hinge line of the aileron was parallel to the leading edge of the wing. The gap between the aileron and wing was sealed with plastecine.

The split flap tested on the model was made of $\frac{1}{16}$-inch sheet steel. The flap had a chord equal to 0.20c and a span equal to one-half the span of the wing. The flap extended across the center section of the model, with the flap hinge line parallel to the leading edge.

Spoilers, also made of $\frac{1}{16}$-inch sheet steel, were tested on the model. The spoiler was mounted forward of the aileron at the 0.70c position on the right wing and extended from the inboard end of the aileron to the wing tip.

For most of the tests the tips of the wings were tips of revolution, but drooped tips were also tested on the 45° swept-back wing. Drooped tips increased the span of the wing to 58 inches. (See figs. 1 and 2(a).)

The model was mounted on the three-strut support and because the angle-of-attack sting for angles of sweepback of 30°, 45°, and 60° was long, a cross bar was required to furnish additional rigidity to the model. (See figs. 2(a) and 2(b).)

TESTS

All the tests were run at a dynamic pressure of 39.7 pounds per square foot. This value corresponds to a Mach number of about 0.165. The Reynolds number varied from about 990,000 to about 1,980,000 because the chord of the wing, measured parallel to the axis of symmetry, was a function of sweep.

For each of the swept-back wings, tests were made at 0° and ±5° yaw. For each of these yaw angles the uncorrected angle of attack was varied from -8° to 26° in 2° increments. For each angle of sweepback, tests were also made at 0° and 10° angle of attack for varying yaw angles. The angles of yaw for these tests were 0°, ±1°, ±2°, ±5°, ±10°, ±15°, ±20°, and ±25°.

The aileron tests were made with angles of 0° and ±15° deflection for each sweepback angle. The split flap tested was set at a deflection of 60°. In each case the angles of deflection were measured in a plane perpendicular to the leading edge of the wing.

Although the spoiler height in inches was constant for most of the tests, the spoiler height in fraction of chord was not constant. For 0° sweep the spoiler deflection was 0.10c, for the 30° swept-back wing the spoiler deflection was 0.087c, for the 45° swept-back wing the spoiler deflections tested were 0.035c and 0.071c, and for the 60° swept-back wing the spoiler deflection was 0.025c.

CORRECTIONS

A static calibration of the model setup was made and the angular deflections of the model due to pitching loads were determined. The data were corrected for the changes in angle of attack caused by pitching moments. No tares were taken for the support struts, angle-of-attack sting, and cross bar.

Since no systematic tunnel corrections for swept-back wings have been investigated, approximate corrections for tunnel-wall effect were applied to the drag and rolling-moment coefficients and to the angle of attack. The following approximate corrections were applied:

$$\Delta C_X = -\delta_W \frac{S}{C} C_{L_t}{}^2$$

$$\Delta \alpha = 57.3\ \delta_W \frac{S}{C} C_{L_t}$$

$$\Delta C_l = K C_{l_t}$$

where

δ_W the boundary correction factor obtained from reference 5

S wing area

C tunnel cross-sectional area, 36 square feet

C_{L_t} uncorrected lift coefficient

C_{l_t} uncorrected rolling-moment coefficient

K a correction factor from reference 6 corrected for application to these tests by taking into account the changes of model and tunnel size

The following table gives values of the correction factors used for each of the swept-back wings:

Λ (deg)	A	S (sq ft)	δ_W	K
0	4.13	2.82	0.147	0.02
0	5.03	3.45	.154	.02
30	4.36	3.98	.154	.02
45	3.56	4.87	.154	.03
45	4.13	5.66	.163	.03
45 (drooped tip)	4.02	5.81	.163	.03
60	2.52	6.89	.154	.03

No corrections were applied to the data to take into account the tunnel-wall effect on the model at large yaw angles when the wing tips were very close to the tunnel

wall. The curves on the figures are shown dashed for that range of yaw angle for which the data probably were most seriously affected by wall interference.

DISCUSSION

The basic data obtained from these tests are presented in figures 3 to 35 and an index of these figures is given in table I. Some results are summarized and compared with theoretical results in figures 36 to 43. A comparison of the data of figures 3 to 35 indicates many differences between the characteristics of a wing with no sweepback and wings with large amounts of sweepback. These differences are particularly noticeable for the variation of lift, pitching moment, and rolling moment with angle of attack.

Plain wings.- The decrease in the slope of the lift curve with sweepback and aspect ratio is shown in figure 36 with an estimated curve.

The maximum lift coefficient of the wings without flaps was approximately independent of the angle of sweepback, but the angle of attack at maximum lift varied nearly inversely as the cosine of the angle of sweepback.

The shape of the curves of lift and pitching moment of the highly swept-back wings as a function of angle of attack are decidedly nonlinear (figs. 3(a), 10(a), and 13(a)). The wing with 60° sweepback at about $C_L = 0.3$ and the wing with 45° sweepback at about $C_L = 0.75$ show an increase in the slope of the lift curve and a diving tendency, indicated by the sudden change in slope of the pitching-moment curve. These characteristics indicate an increase in load at the tips, possibly accompanied by a rearward shift of the center of pressure at each section. Tuft observation at this attitude indicates the air flow to be rough and nearly parallel to the wing leading edge near the root and center parts of the wing. At higher angles of attack the expected tip-stalling tendency of swept-back wings was encountered; this tendency is indicated by the rounding of the lift curve, by the unstable slope of the pitching-moment curve, and by large increases in drag. The longitudinal-force coefficient near $C_{L_{max}}$ is at least 5 times as great for the wing with 60° sweepback as for the unswept wing (figs. 3(b) and 27(b)). The

increased chord of the drooped tips on the wing with 45° sweepback had no appreciable effect on the unstable pitching-moment slope caused by tip stalling (fig. 11(a)).

Data from tests at about the same Reynolds number and Mach number (0.1) in the Langley 300 MPH 7- by 10-foot tunnel of a semispan model of a 60° swept-back, tapered wing have shown qualitatively these same lift and pitching-moment characteristics. The wings with 0° and 30° sweepback did not show the unusual effects encountered with wings of 45° and 60° sweepback. The 30° swept-back wing, however, did have a diving tendency just before the stall (fig. 20(a)). The value of C_L at which irregularities occur is a linear function of sweepback, as are the values of C_L at which tip stalling is indicated by the abrupt positive change in the slope of the pitching-moment curve (fig. 43).

The adverse effects on longitudinal stability of plain wings caused by large amounts of sweepback are shown by the curves of aerodynamic center as a function of lift coefficient (fig. 37). The curves for the 45° and 60° swept-back wings indicate that further investigation is necessary in order to find ways of reducing the large neutral-point shifts shown by these data.

The lift of the unswept wings decreased markedly when yawed, but as the angle of sweepback was increased the lift remained more nearly constant as the wing was yawed. For the 60° swept-back wing the lift was nearly independent of angle of yaw (fig. 5(a)).

The rolling moment of the swept-back wings when yawed increased nearly linearly with lift coefficient in the direction to raise the forward wing until the critical lift coefficients were reached. The forward wing apparently stalled first when yawed at high lift coefficients, as indicated by the decrease in the rolling moment that tended to raise the forward wing. (For example, fig. 3(c).)

The rate of change of rolling-moment coefficient with angle of yaw C_{l_ψ} was small and nearly the same at zero lift coefficient for all wings tested (fig. 38). The value of C_{l_ψ}, however, increased at a different rate with lift coefficient for each wing tested. All the swept-back wings with flaps neutral reached a maximum value of C_{l_ψ} of about 0.004, which value in terms of a conventional

unswept wing of aspect ratio 6 corresponds to about 20° effective dihedral. The rates of change of C_{l_ψ} with lift coefficient measured at small lift coefficients (from the curves of fig. 38) are plotted against angle of sweepback in figure 39 with an estimated curve.

The value of $\partial C_{l_\psi}/\partial C_L$ for the unswept wing (0.001) probably can be attributed to the effects of the nearly blunt tip shapes (reference 7). Of the total value of $\partial C_{l_\psi}/\partial C_L$ for the swept-back wings, possibly $\Delta\left(\partial C_{l_\psi}/\partial C_L\right) = 0.001$ may be attributed to the effects of tip shape.

The drooped tips tested on the 45° swept-back wing acted somewhat as a low-aspect-ratio surface with negative dihedral and thereby reduced the values of C_{l_ψ} by about 0.0006 at $C_L \cong 0.1$ and by about 0.0014 at $C_L \cong 0.7$ (for drooped tip 2). (See fig. 12(c).) The unfavorable lateral-stability characteristics of wings with large sweepback can be reduced by the use of a drooped tip because the drooped tip decreased C_{l_ψ} in proportion to an increase in C_L.

The side force and yawing moments change rapidly and irregularly when the wing is yawed at lift coefficients greater than the critical values when the diving moment occurs. At small lift coefficients the directional stability C_{n_ψ} is small but favorable, except for the 60° swept-back wing at negative C_L, and increases as some power greater than the first power of the absolute value of the lift coefficient; this increase indicates that the yawing moment is caused mainly by the differences in drag of the two sides of the wing when yawed. The drooped tips increased the directional stability of the wing with 45° sweepback at small lift coefficients but had no appreciable effect at large lift coefficients (fig. 12(c)).

Ailerons.- The effectiveness of a half-span 0.20c aileron on each of the various wings tested is indicated in figure 40 by the slopes measured between ±15° aileron deflection for $C_L = 0.2$. Similar variations can be expected up to a lift coefficient of 0.5. The marked decrease in aileron effectiveness with sweepback combined

with the marked increase in C_{l_ψ} indicates that with highly swept-back wings the ailerons cannot trim out the rolling moment caused by large angles of yaw. For example, these data indicate that 30° total aileron angle would be capable of trimming only 2°, 6°, 9°, and 32° angle of yaw for the 60°, 45°, 30°, and 0° swept-back wings, respectively, at the lift coefficients corresponding to maximum C_{l_ψ} with flaps neutral (fig. 38). The curves of figures 5(c), 15(c), 22(c), and 29(c) show that as the angle of sweepback is increased, the aileron on the rearward wing when yawed becomes progressively less effective in producing rolling moment and the aileron on the forward wing becomes more effective. For the 45° and 60° swept-back wings the aileron on the rearward wing when yawed becomes relatively ineffective. Upward deflection of the aileron on either wing appreciably reduces the slope C_{l_ψ}.

Because C_{L_α} and $C_{l_{\delta_a}}$ decrease with increases in sweep the damping in roll could also be expected to decrease. The ailerons therefore may be capable of producing satisfactory rates of roll on highly swept-back wings.

The small change in pitching moment caused by aileron deflection indicates that wing-tip elevators having swept-back hinge lines would be relatively ineffective on highly swept-back wings.

Spoilers.- The effectiveness, in producing rolling moment, of nearly half-span spoilers located at 0.7c on the upper surface of the wing is summarized in figure 41. For the wing with an angle of sweepback of 60°, the 0.025c spoiler produced rolling moment in the wrong direction. The ineffectiveness of the spoiler on the swept-back wings in producing rolling moment is probably associated with a very thick boundary layer near the tip of the highly swept-back wings compared with that of the unswept wing.

The spoiler produced characteristics similar to those of the aileron with regard to the variation of effectiveness with yaw; that is, the spoiler on the highly swept-back wings was totally ineffective on the rearward wing but more effective than at zero yaw when on the forward wing.

The rather large and favorable yawing moments produced by spoiler deflection suggest the use of a spoiler as a directional control device. Rolling moments can be produced by spoiler action indirectly by causing favorable sideslip.

Split flaps.- The effectiveness of half-span 0.20c split flaps deflected 60° in changing the lift at 0° angle of attack and in producing an increment in maximum lift is indicated in figure 42. The estimated curves (dashed curves of fig. 42) show that the flap is producing about all the increment in C_L at 0° angle of attack that can be expected. The flap produced no increment in $C_{L_{max}}$ for the wing with 60° sweepback. In fact, the flap may even produce a decrease in $C_{L_{max}}$ not indicated by the data obtained. Maximum lift of the 60° swept-back wing without flap was not obtained because of limitations of the apparatus. The value of C_L at moderate angles of attack was, however, appreciably increased by deflection of the split flaps.

For the swept-back wings, deflection of the flap did not appreciably change the value of C_{l_ψ} at small values of C_L but at high values of C_L the value of C_{l_ψ} was changed considerably. At large values of C_L the one value obtained with flap deflected and the wing at approximately 11° angle of attack indicated values of C_{l_ψ} of 0.0046 for the 30° and 0.0055 for the 45° and the 60° swept-back wings (fig. 38).

On the wings with 30°, 45°, and 60° sweepback the split flap tested was nearly self trimming in pitch. The slopes of the pitching-moment curve throughout the lift range were not appreciably altered by deflection of the split flap.

Estimated characteristics.- The simple concepts suggested in reference 1 have been used to estimate certain characteristics of the swept-back wings from the measured characteristics of the unswept wing. These concepts involve the assumption that changes in sweepback angle, obtained by pivoting the semispan of a given wing about an axis in the plane of symmetry, affect the loading over each semispan only insofar as sweep affects the components of velocity normal to the leading edge and

the angles of attack of these velocity components with respect to the planes of the wing semispans. When the wings are swept back in the manner indicated (that is, the areas of the wing panels and the span measured parallel to the leading edge are maintained constant), the following characteristics are indicated:

$$C_{L_\alpha} = \left(C_{L_\alpha}\right)_{\Lambda=0} \cos \Lambda$$

$$C_{l_{\delta_a}} = \left(C_{l_{\delta_a}}\right)_{\Lambda=0} \cos^2 \Lambda$$

and for a given split flap or spoiler deflection

$$\Delta C_L = \left(\Delta C_L\right)_{\Lambda=0} \cos^2 \Lambda$$

$$\Delta C_l = \left(\Delta C_l\right)_{\Lambda=0} \cos^2 \Lambda$$

The areas of the wings used in the present investigation were increased by extending the wing tips in order to maintain constant span as the angle of sweepback was increased. In order to apply the concepts of reference 1 consistently, therefore, it seems reasonable to correct the data for the unswept wing tested to the aspect ratio of unswept wings having the same wing-panel plan form as the swept-back wings, as well as to correct for the effects of sweep on wings of constant wing-panel plan form. On this basis, the following equations may be written (the planes in which the variables are measured being taken into account):

$$C_{L_\alpha} = \left(C_{L_\alpha}\right)_{\Lambda=0} \eta \cos \Lambda$$

$$C_{l_{\delta_a}} = \left(C_{l_{\delta_a}}\right)_{\Lambda=0} \eta' \cos^2 \Lambda$$

and for a given split flap or spoiler deflection

$$\Delta C_L = \left(\Delta C_L\right)_{\Lambda=0} \eta \cos^2 \Lambda$$

$$\Delta C_l = \left(\Delta C_l\right)_{\Lambda=0} \eta' \cos^2 \Lambda$$

in which the factors η and η' are defined as follows:

$$\eta = \frac{\left(\frac{A}{E_e A + 2}\right)_0}{\left(\frac{A}{E_e A + 2}\right)_{\Lambda=0}}$$

$$\eta' = \frac{\left(\frac{A}{E'_e A + 4}\right)_0}{\left(\frac{A}{E'_e A + 4}\right)_{\Lambda=0}}$$

In the foregoing factors the subscript 0 refers to unswept wings having the same wing-panel shape as the swept-back wings, and the subscript $\Lambda = 0$ refers to the wing tested with zero sweepback. The factors E_e and E'_e are the effective edge-velocity correction factors for angle-of-attack loading and for rolling moment, respectively. (See reference 4.)

The estimated characteristics are indicated by the dashed curves of figures 36, 40, 41, and 42. Inspection of figures 36, 40, and 42 shows that the experimental data for the slope of the lift curve C_{L_α}, the aileron effectiveness $C_{l_{\delta_a}}$, and the split flap effectiveness $(\Delta C_L)_{\alpha=0}$ were slightly lower than the estimated curves. This variation indicates that the velocity-component concept underestimates the effects of sweep on these

characteristics. The increment of rolling moment caused by spoiler deflection (fig. 41) decreased much faster with sweep than the estimated curve. This variation is probably attributable to the fact that the boundary layer is carried toward the tip as the sweepback is increased and also to the decrease in effective spoiler deflection with sweepback.

By means of the previously discussed concepts, Betz (reference 1) derived an expression for the rolling-moment coefficient caused by sideslip as affected by sweep. In Betz's analysis, however, the type of sweep considered was one in which the leading edge of the swept wing was maintained in a horizontal plane regardless of the angle of attack of the wing. This type of sweep represents a condition in which the angle between the planes of the left and right semispan wings (dihedral angle) varies with angle of attack and does not apply therefore to the configurations of the wings considered in the present investigation (that is, wings swept in a manner such that the angle between the planes of the right and left semispan wings is maintained at 180°, or zero dihedral, regardless of the angle of attack). An equation, based on the same simplified assumptions made by Betz (reference 1), has been derived to apply to the wings (swept in the manner just discussed) of the present investigation. This equation, which gives values of C_{l_ψ} equal to one-half those obtained by Betz, is as follows:

$$C_{l_\psi} = \frac{1}{57.3} \frac{C_L}{4} \tan \Lambda$$

The dashed curve of figure 39 was obtained by adding to the value of $\partial C_{l_\psi}/\partial C_L$ caused by sweep, as determined by the relationship just given, the experimental value of $\left(\partial C_{l_\psi}/\partial C_L\right)_{\Lambda=0}$. The agreement between the experimental and estimated curves is good but may be fortuitous because of the assumptions made in the derivation of the theoretical relationship.

CONCLUSIONS

Results of tests in the Langley stability tunnel of untapered constant-span wings having angles of sweepback

of 0°, 30°, 45°, and 60° indicated the following effects of sweepback on stability and control characteristics:

1. Large changes in longitudinal stability occurred at moderately large lift coefficients for the wings with 45° and 60° sweepback.

2. The rate of change of rolling-moment coefficient with angle of yaw increased with lift coefficient and nearly as the tangent of the angle of sweepback. All the swept-back wings with flaps neutral reached a maximum value of rate of change of rolling-moment coefficient with angle of yaw of about 0.004. With flaps deflected rate of change of rolling-moment coefficient with angle of yaw increased to about 0.0055 at some lift coefficient.

3. Drooping the wing tips decreased the rate of change of rolling-moment coefficient with angle of yaw, and the reduction increased with increase in lift coefficient. Drooping the tips appeared to be a promising means of reducing the unfavorable lateral-stability characteristics of wings with large sweepback.

4. Aileron effectiveness as measured by the slope of the curve of rolling-moment coefficient plotted against aileron angle decreased with angle of sweepback about as much as would be expected from simple theoretical considerations. This fact combined with the large increase in lateral stability with sweepback indicated that, with highly swept-back wings, the aileron cannot trim out the rolling moment caused by large angles of yaw.

5. The small change in pitching moment caused by aileron deflection indicated that wing-tip elevators having swept-back hinge lines would be relatively ineffective on highly swept-back wings.

6. The maximum lift coefficient of the wings without flaps was approximately independent of the angle of sweepback, but the angle of attack at maximum lift varied nearly inversely as the cosine of the angle of sweepback.

7. The split-flap effectiveness at 0° angle of attack decreased with sweepback. The increment of maximum lift coefficient with flaps deflected decreased with increase in sweepback and the maximum lift coefficient for the 60° swept-back wing may be less than that with flap neutral.

8. Spoiler effectiveness in producing rolling moments decreased with sweepback much faster than would be indicated by the simple theory. The large and favorable yawing moments produced by the spoiler indicated that spoilers may be of some use in directional control.

Langley Memorial Aeronautical Laboratory
National Advisory Committee for Aeronautics
Langley Field, Va., March 26, 1946

REFERENCES

1. Betz, A.: Applied Airfoil Theory. Unsymmetrical and Non-Steady Types of Motion. Vol. IV of Aerodynamic Theory, div. J, ch. IV, sec. 4, W. F. Durand, ed., Julius Springer (Berlin), 1935, pp. 102-107.

2. Munk, Max M.: Note on the Relative Effect of the Dihedral and the Sweep Back of Airplane Wings. NACA TN No. 177, 1924.

3. Jones, Robert T.: Wing Plan Forms for High-Speed Flight. NACA TN No. 1033, 1946.

4. Swanson, Robert S., and Priddy, E. LaVerne: Lifting-Surface-Theory Values of the Damping in Roll and of the Parameter Used in Estimating Aileron Stick Forces. NACA ARR No. L5F23, 1945.

5. Silverstein, Abe, and White, James A.: Wind-Tunnel Interference with Particular Reference to Off-Center Positions of the Wing and to the Downwash at the Tail. NACA Rep. No. 547, 1935.

6. Swanson, Robert S.: Jet-Boundary Corrections to a Yawed Model in a Closed Rectangular Wind Tunnel. NACA ARR, Feb. 1943.

7. Shortal, Joseph A.: Effect of Tip Shape and Dihedral on Lateral-Stability Characteristics. NACA Rep. No. 548, 1935.

TABLE I - INDEX OF FIGURES

Figure	Angle of sweepback, Λ (deg)	Aspect ratio A	Model configuration	Data plotted against
3	60	2.52	Plain wing	α
4	60	2.52	Wing + aileron	α
5	60	2.52	Wing + aileron	ψ
6	60	2.52	Wing + spoiler	α
7	60	2.52	Wing + spoiler	ψ
8	60	2.52	Wing + split flap	α
9	60	2.52	Wing + split flap	ψ
10	45	4.13	Plain wing	α
11	45	4.02	Wing + drooped tips	α
12	45	4.02	Wing + drooped tips	ψ
13	45	3.56	Plain wing	α
14	45	3.56	Wing + aileron	α
15	45	3.56	Wing + aileron	ψ
16	45	3.56	Wing + spoiler	α
17	45	3.56	Wing + spoiler	ψ
18	45	3.56	Wing + split flap	α
19	45	3.56	Wing + split flap	ψ
20	30	4.36	Plain wing	α
21	30	4.36	Wing + aileron	α
22	30	4.36	Wing + aileron	ψ
23	30	4.36	Wing + spoiler	α
24	30	4.36	Wing + spoiler	ψ
25	30	4.36	Wing + split flap	α
26	30	4.36	Wing + split flap	ψ
27	0	5.03	Plain wing	α
28	0	5.03	Wing + aileron	α
29	0	5.03	Wing + aileron	ψ
30	0	5.03	Wing + spoiler	α
31	0	5.03	Wing + spoiler	ψ
32	0	5.03	Wing + split flap	α
33	0	5.03	Wing + split flap	ψ
34	0	4.13	Plain wing	α
35	0	4.13	Plain wing	ψ

NATIONAL ADVISORY
COMMITTEE FOR AERONAUTICS

Λ (deg)	A	b (in.)	$\bar{c}$ (in.)	$\bar{x}$ (in.)	Spoiler span (in.)
0	4.13	40.92	9.88	2.48	- - - - - -
0	5.03	50.00	9.89	2.49	12.5
30	4.36	50.00	11.45	10.05	11.5
45 (drooped tip)	4.02	58.00	14.34	18.32	- - - - - -
45	3.56	50.00	14.02	15.94	10.5
45	4.13	58.00	14.04	17.94	- - - - - -
60	2.52	50.00	19.82	26.45	10.8

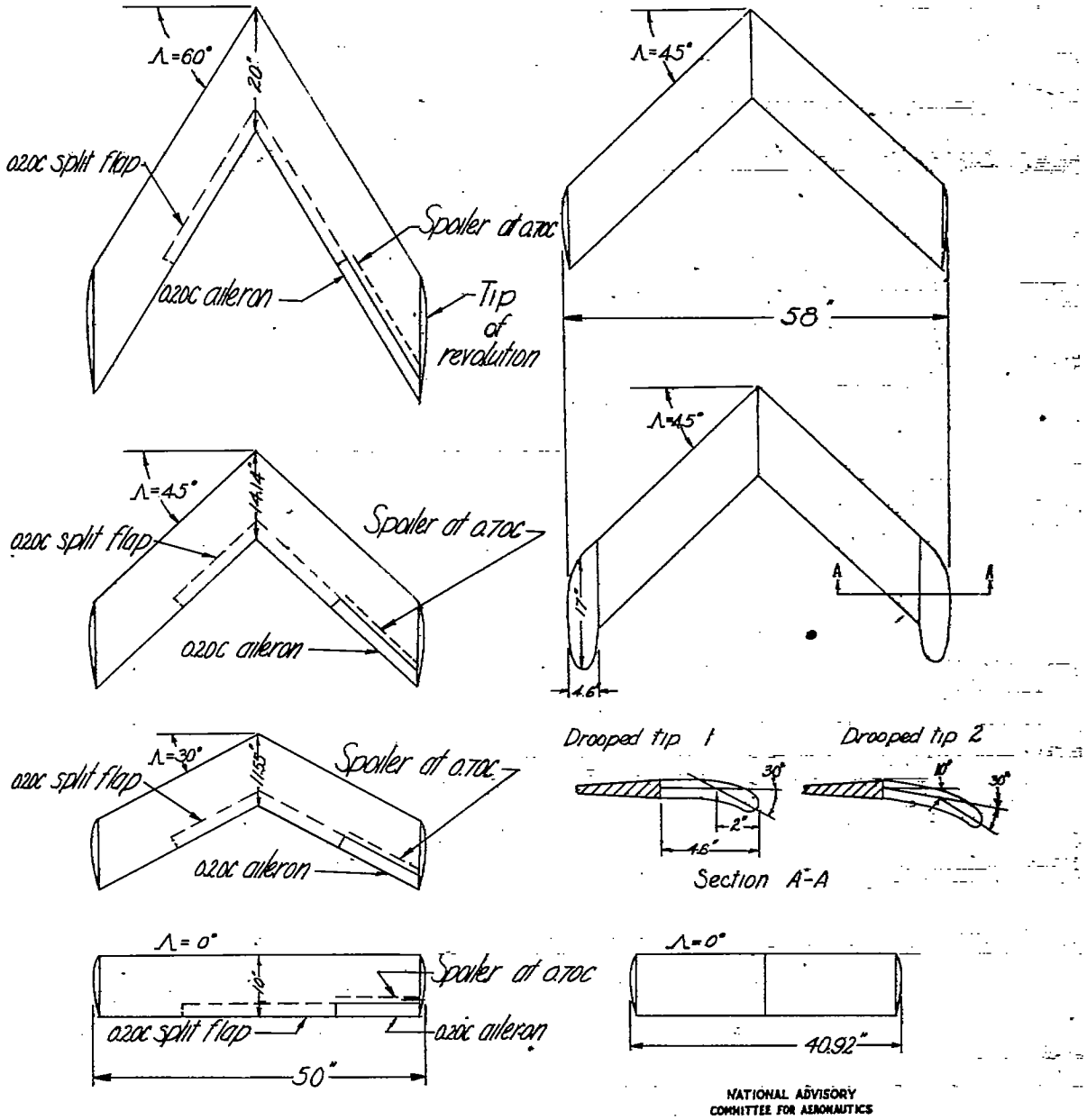

NATIONAL ADVISORY COMMITTEE FOR AERONAUTICS

Figure 1.-Plan forms of swept-back wings.

(a) Downstream view of 45° swept-back wing with drooped tip.

Figure 2.- Swept-back wings mounted on three-strut supports in the Langley stability tunnel.

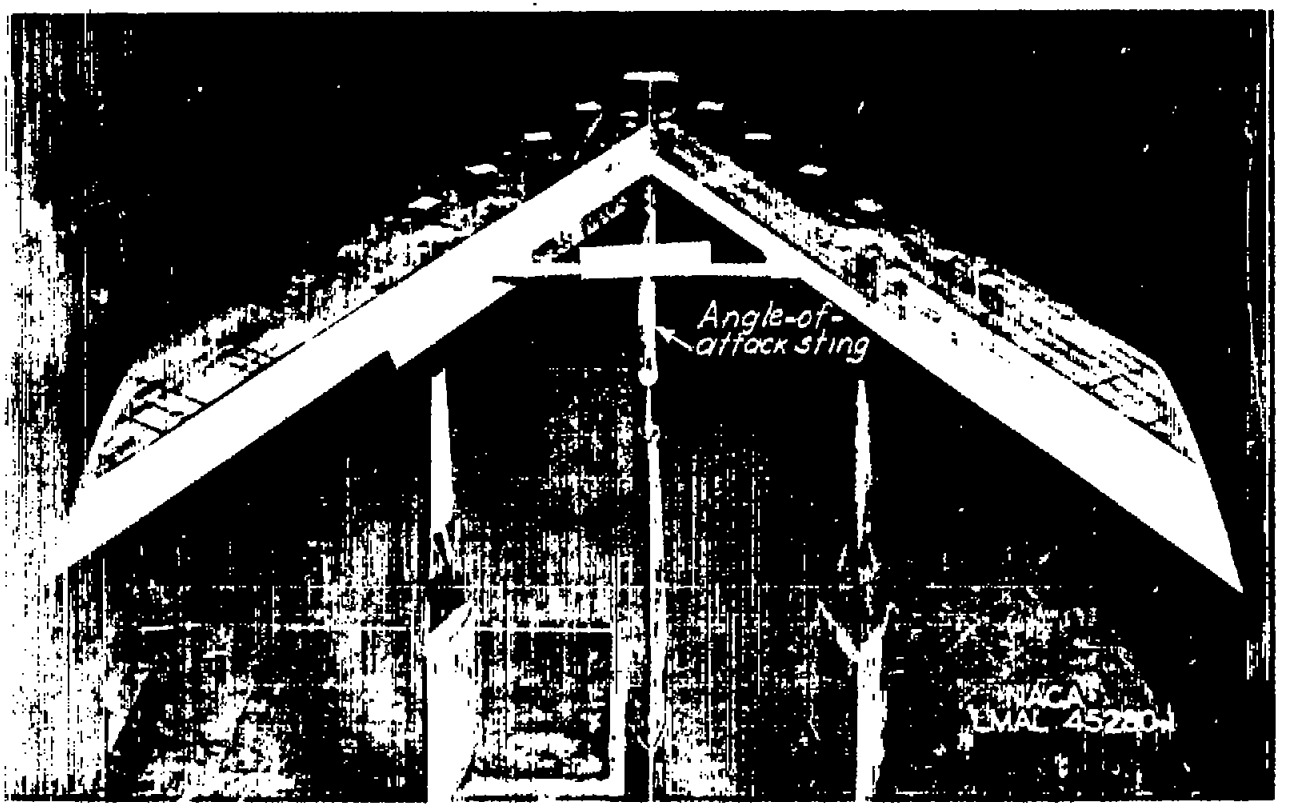

(b) Upstream view of 60° swept-back wing with split flaps.

Figure 2.- Concluded.

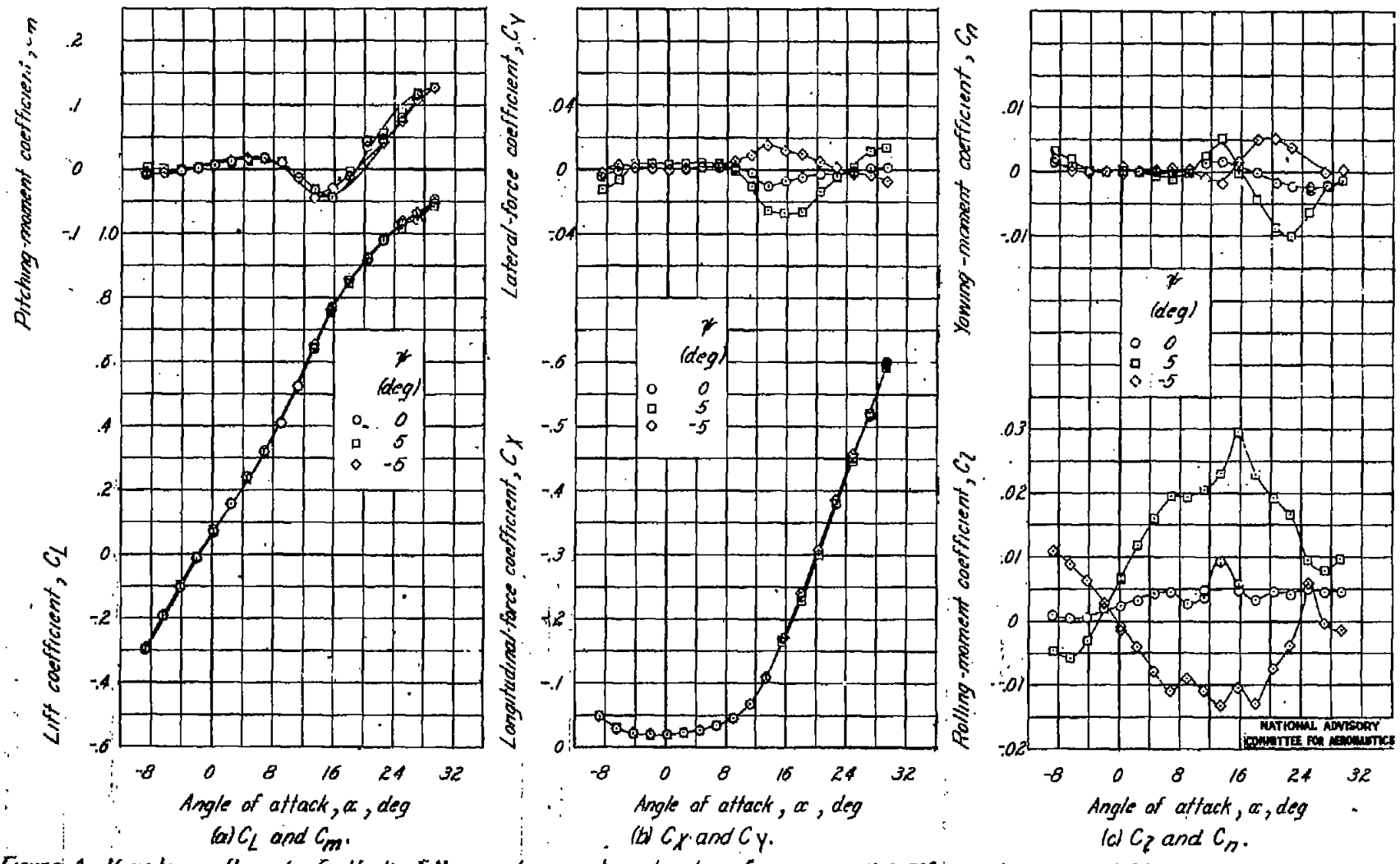

(a) C_L and C_m. (b) C_X and C_Y. (c) C_l and C_n.

Figure 3.- Variation with angle of attack of the aerodynamic characteristics of a rectangular 60° swept-back wing. A,2.52.

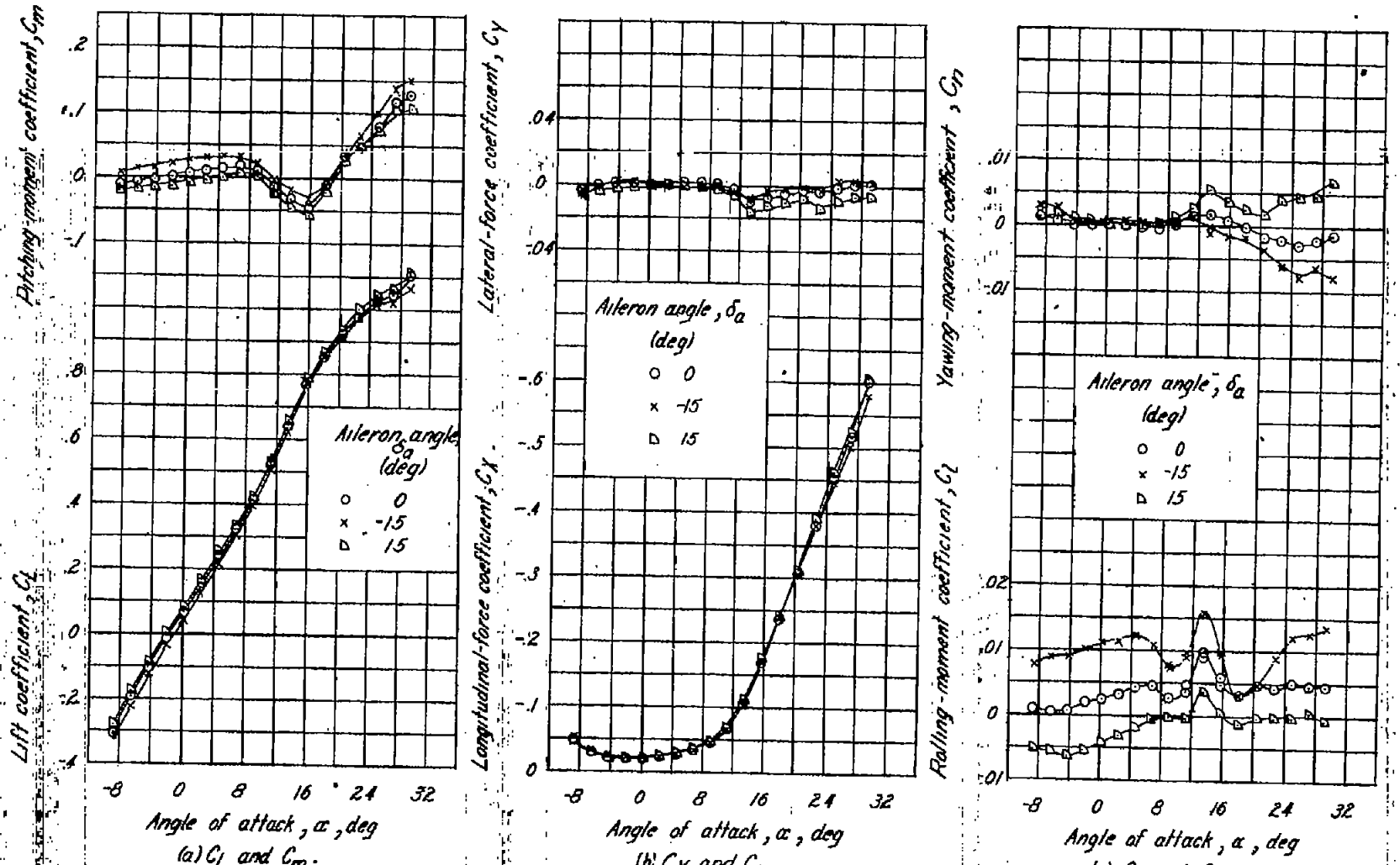

Figure 4.- Variation with angle of attack of the aerodynamic characteristics of a rectangular 60° swept-back wing with a 0.20c chord, 0.50b/2 span aileron on the right wing. A, 2.52.

NATIONAL ADVISORY COMMITTEE FOR AERONAUTICS.

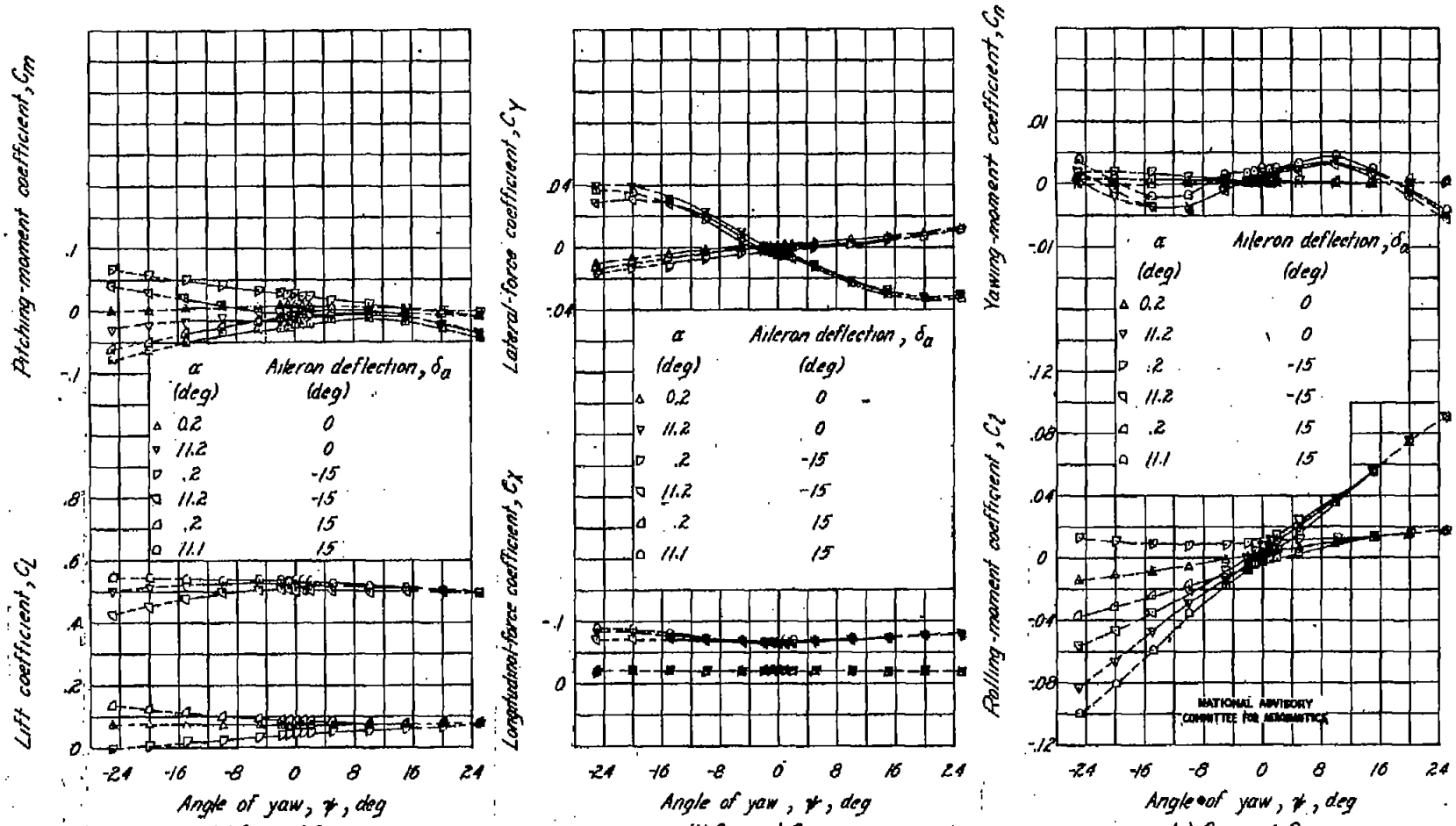

(a) C_L and C_m. (b) C_X and C_Y. (c) C_l and C_n.

Figure 5.- Variation with angle of yaw of the aerodynamic characteristics of a rectangular 60° swept-back wing with a 0.20c chord, 0.50b/2 span aileron on the right wing. A, 2.52.

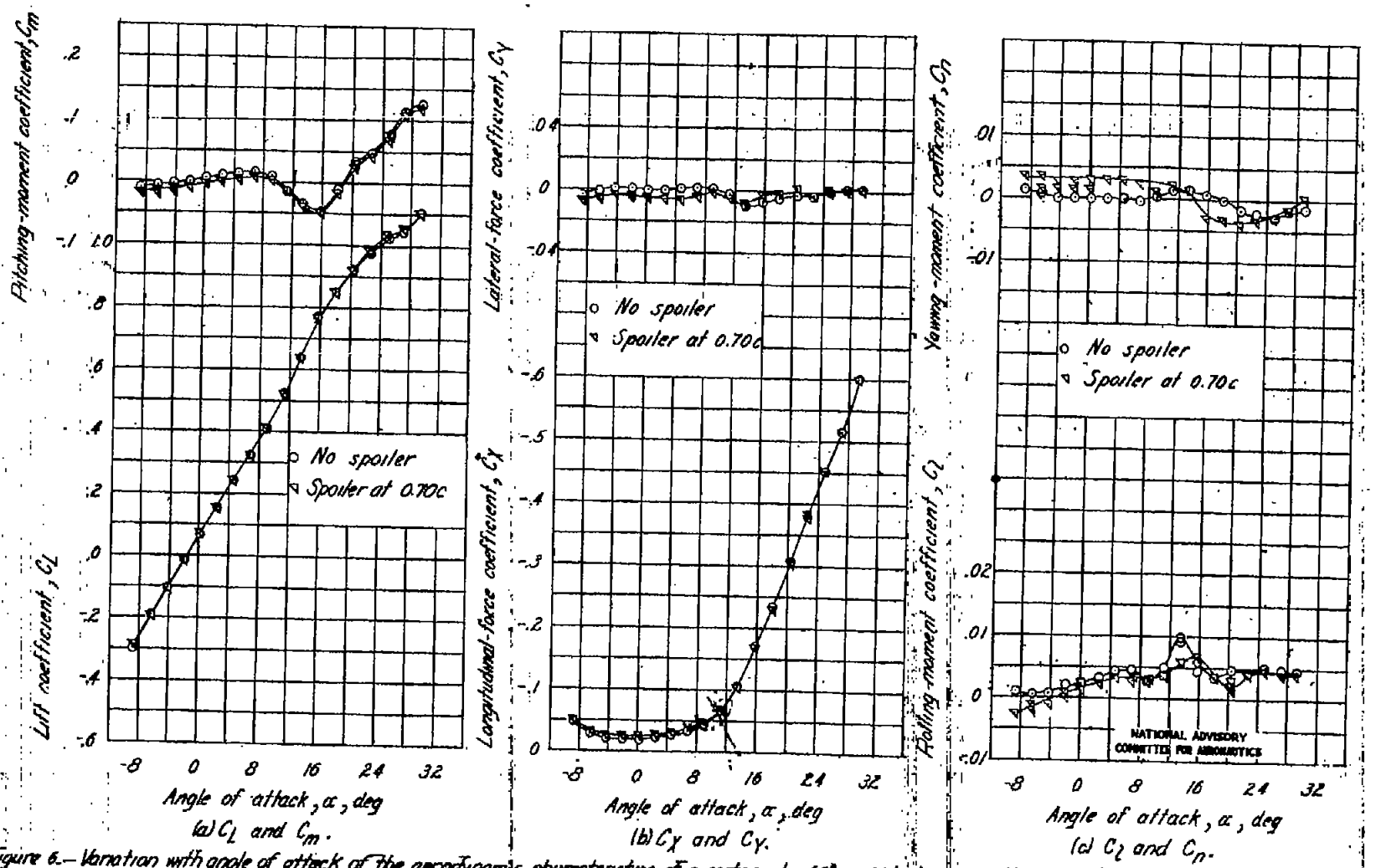

Figure 6.– Variation with angle of attack of the aerodynamic characteristics of a rectangular 60° swept-back wing with a 0.43b/2 span spoiler deflected 0.025c on right wing. A, 2.52.

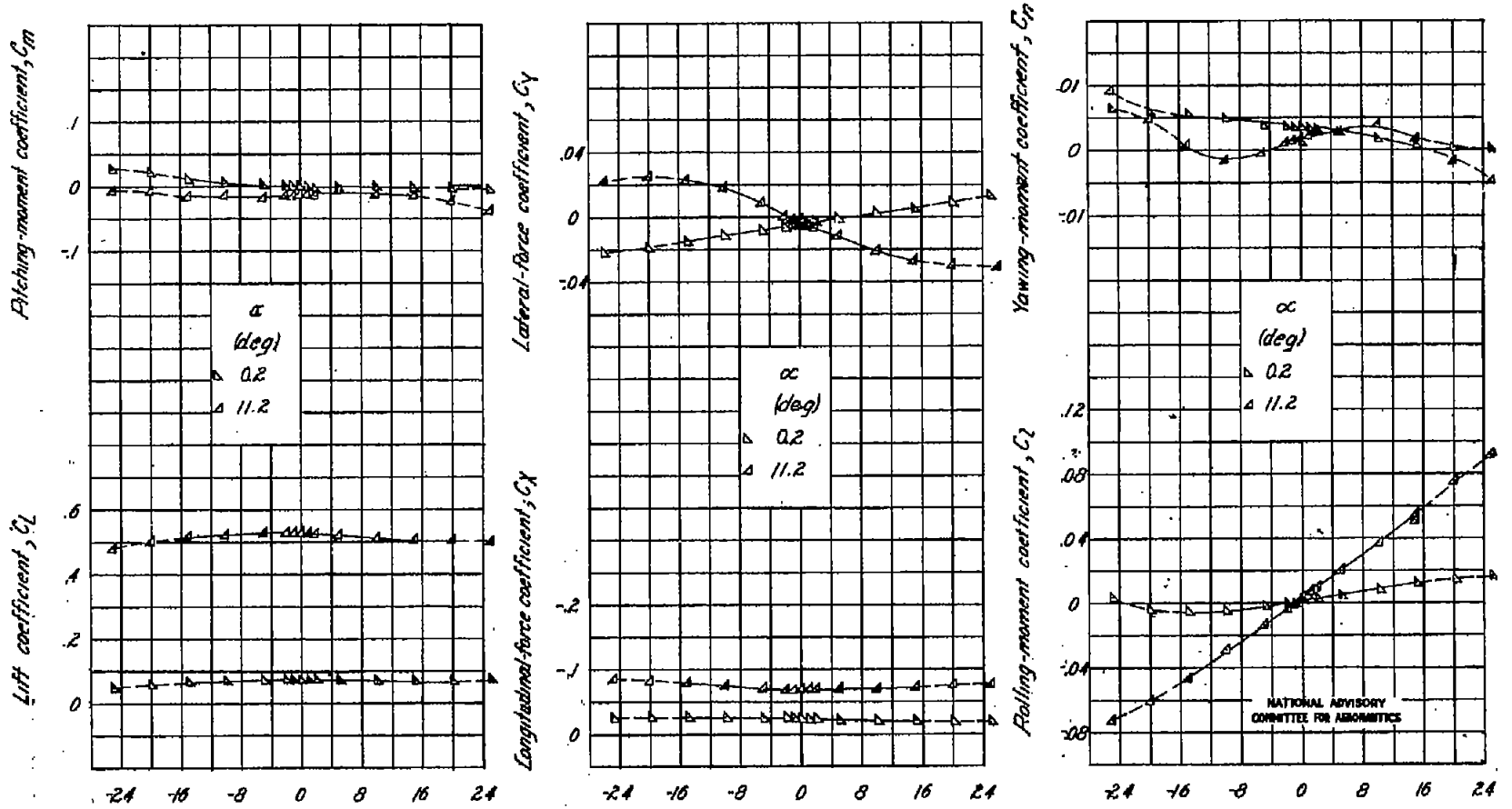

Figure 19.–Variation with angle of yaw of the aerodynamic characteristics of a rectangular 60° sweptback wing with a 0.43 $\frac{b}{2}$ span spoiler deflected 0.025c on right wing. A, 2.32.

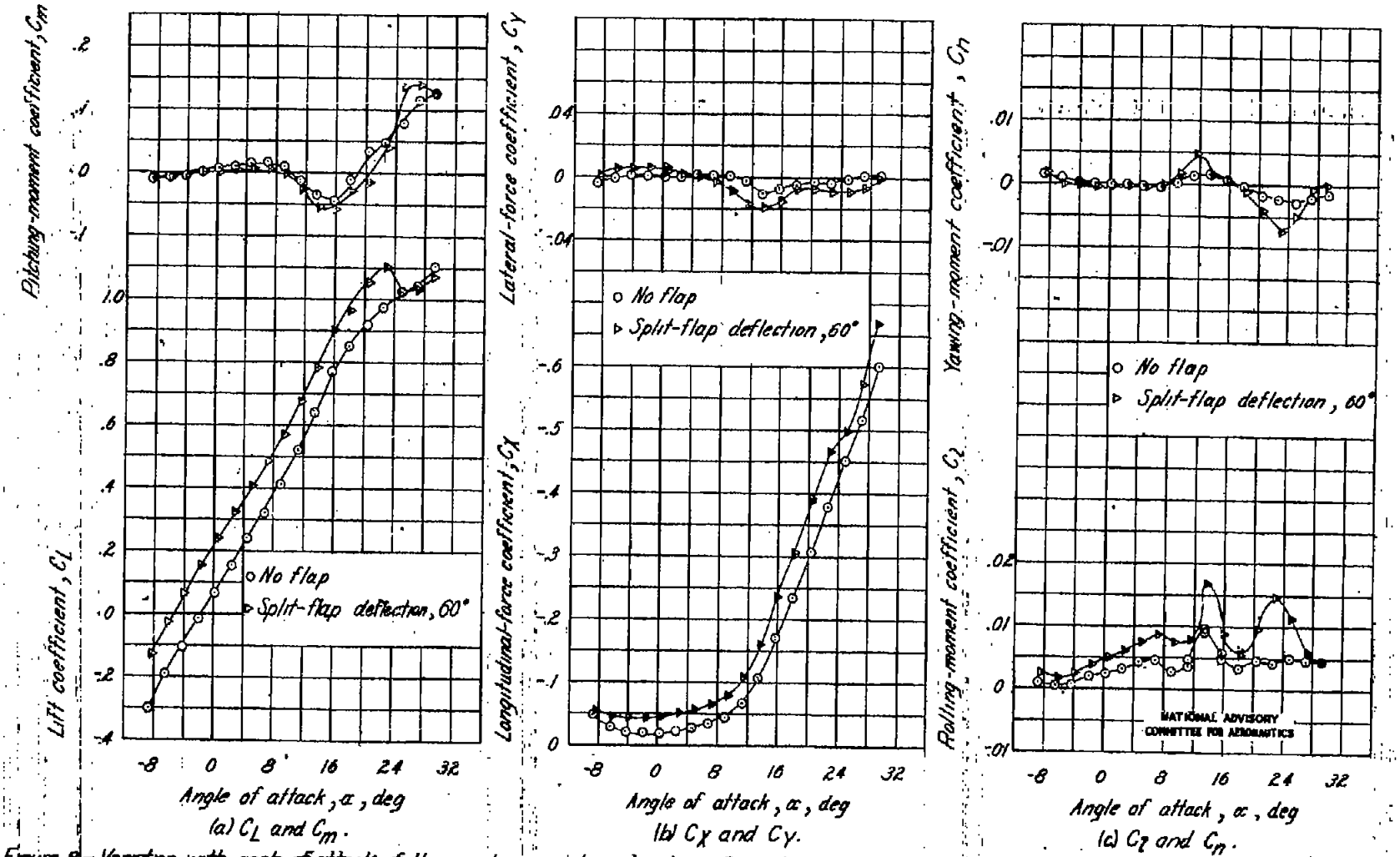

Figure 8.- Variation with angle of attack of the aerodynamic characteristics of a rectangular 60° swept-back wing with a 0.20c chord, 0.50b span split flap deflected 60°. A, 2.52.

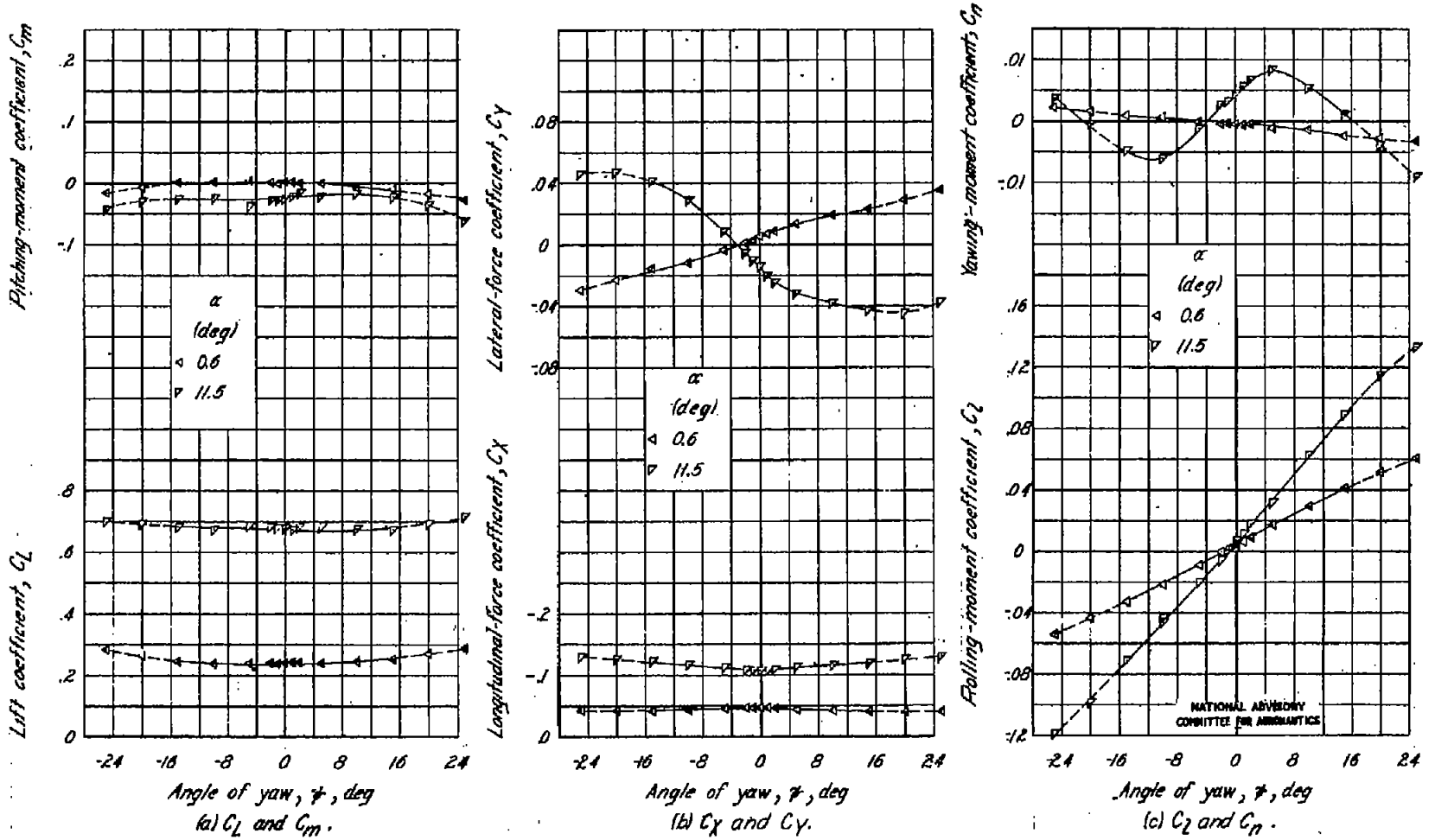

Figure 9.- Variation with angle of yaw of the aerodynamic characteristics of a rectangular 60° swept-back wing with a 0.20c chord, and 0.50b span split flap deflected 60°. A, 2.52.

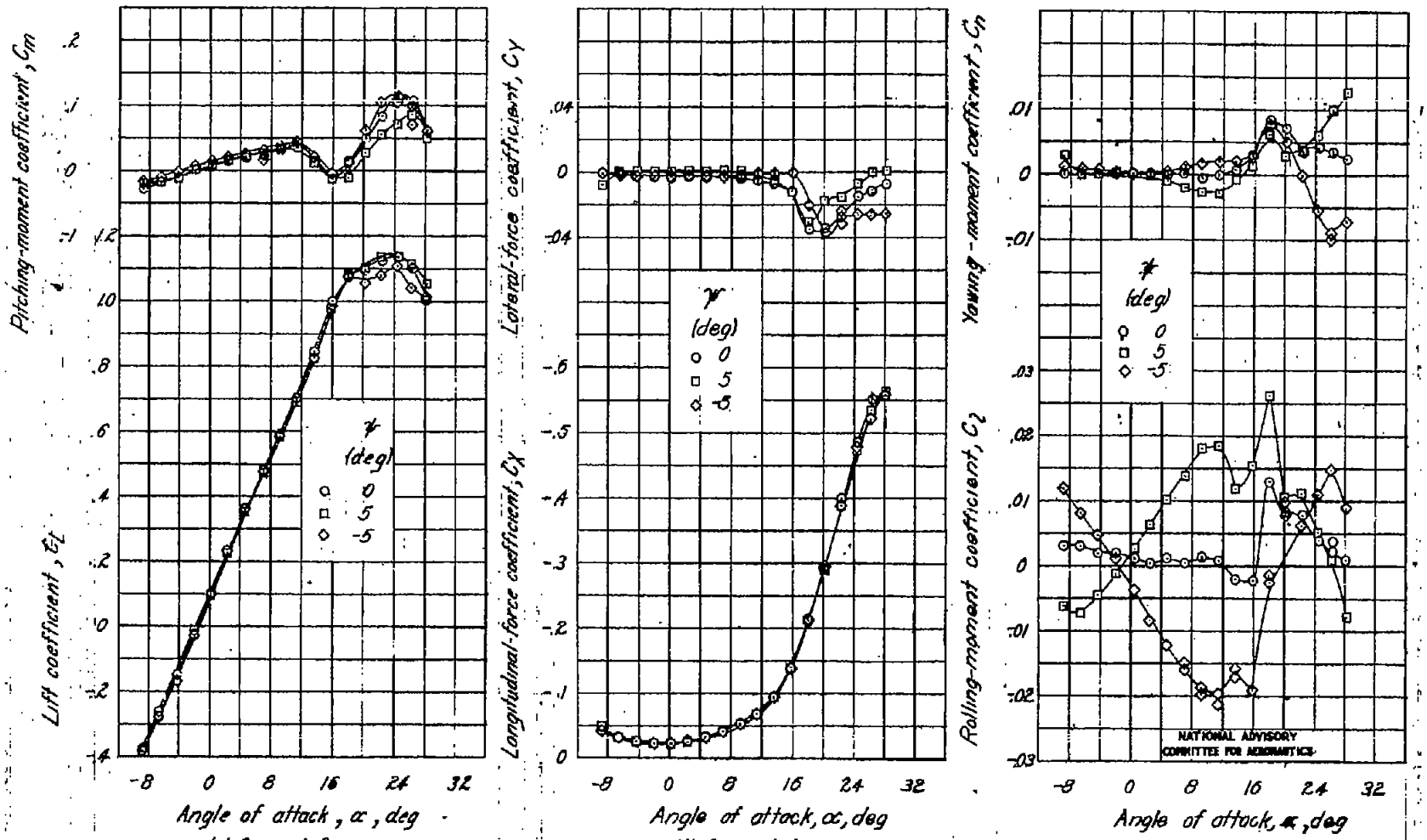

(a) C_L and C_m. (b) C_X and C_Y. (c) C_l and C_n.

Figure 10.-Variation with angle of attack of the aerodynamic characteristics of a rectangular 45° swept-back wing. AR 3.

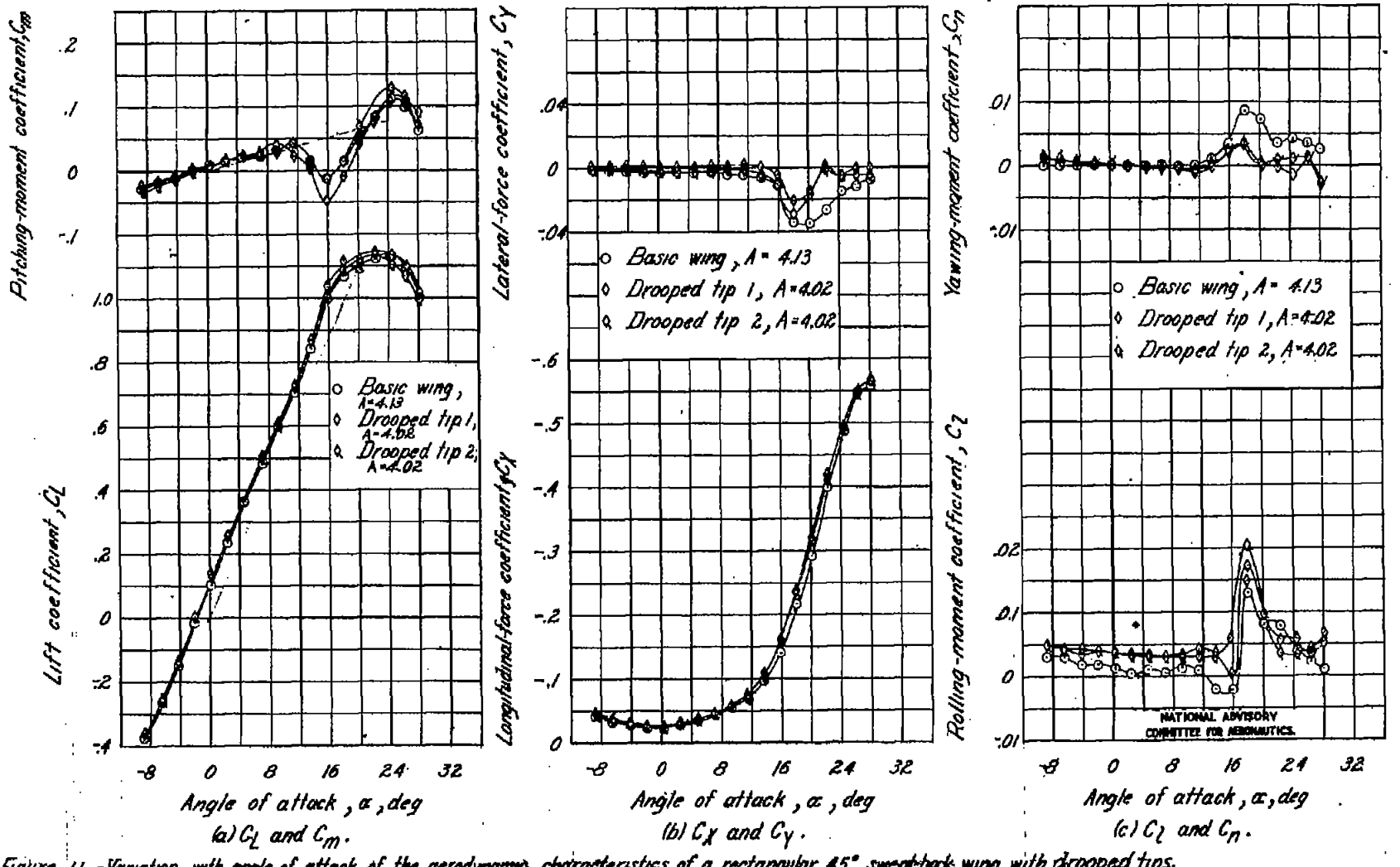

Figure 11.-Variation with angle of attack of the aerodynamic characteristics of a rectangular 45° swept-back wing with drooped tips.

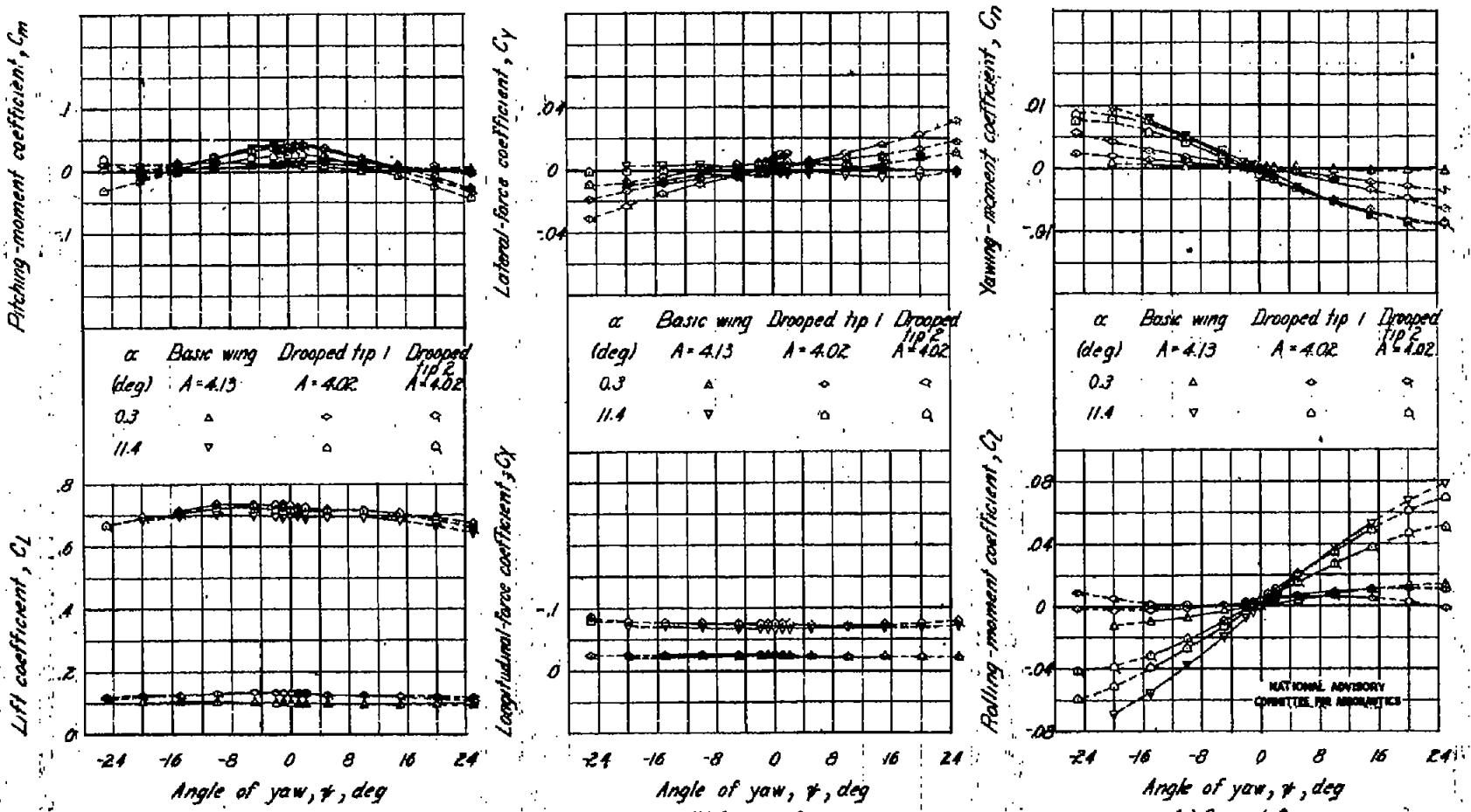

(a) C_L and C_m. (b) C_X and C_Y. (c) C_l and C_n.

Figure 12-Variation with angle of yaw of the aerodynamic characteristics of a rectangular 45° swept-back wing with drooped tips.

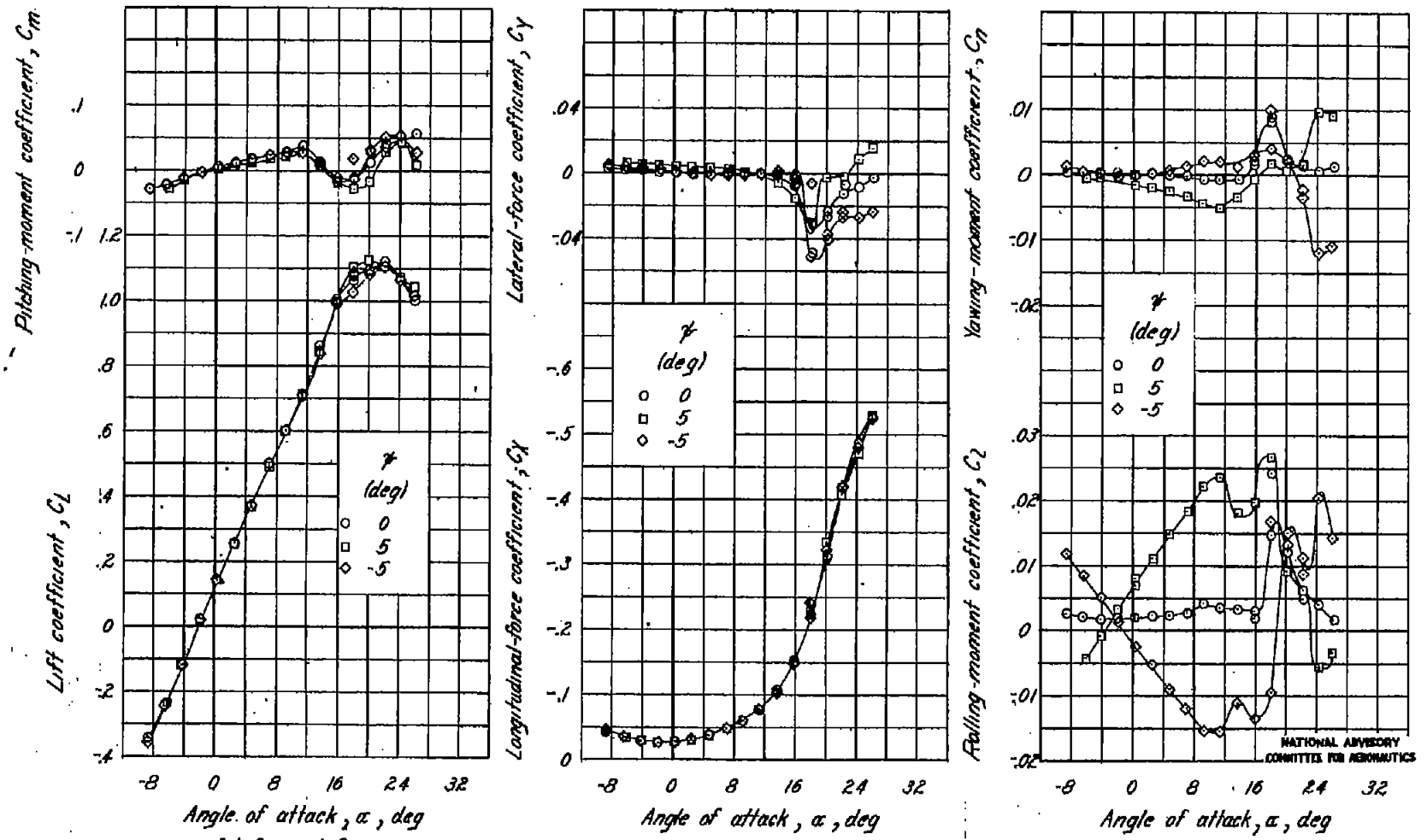

Figure 13.-Variation with angle of attack of the aerodynamic characteristics of a rectangular 45° swept-back wing. A,356.

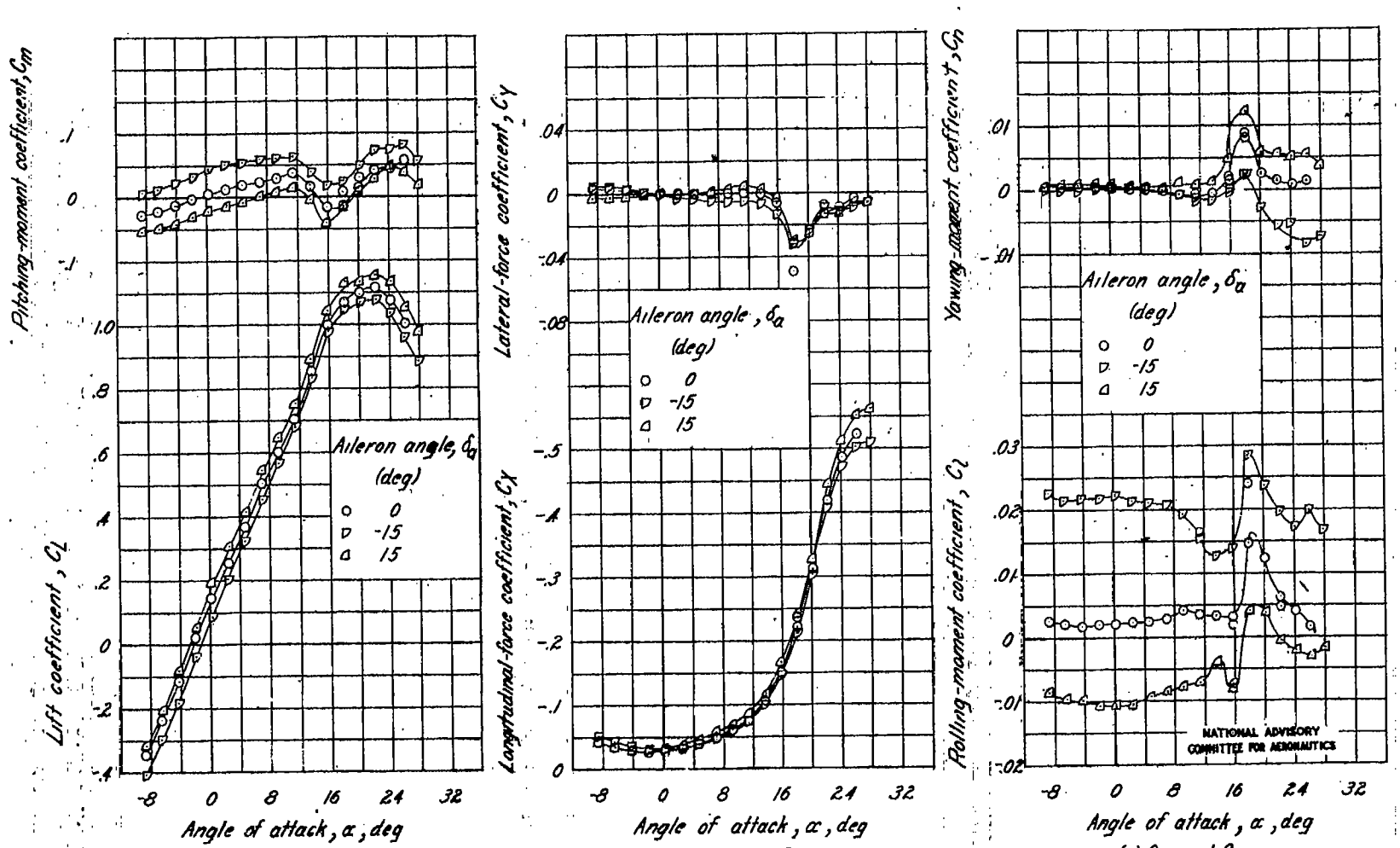

(a) C_L and C_m.

(b) C_X and C_Y.

(c) C_l and C_n.

Figure 14.-Variation with angle of attack of the aerodynamic characteristics of a rectangular 45° swept-back wing with a 0.20c chord, 0.50b/2 span aileron on the right wing. A, 3.56.

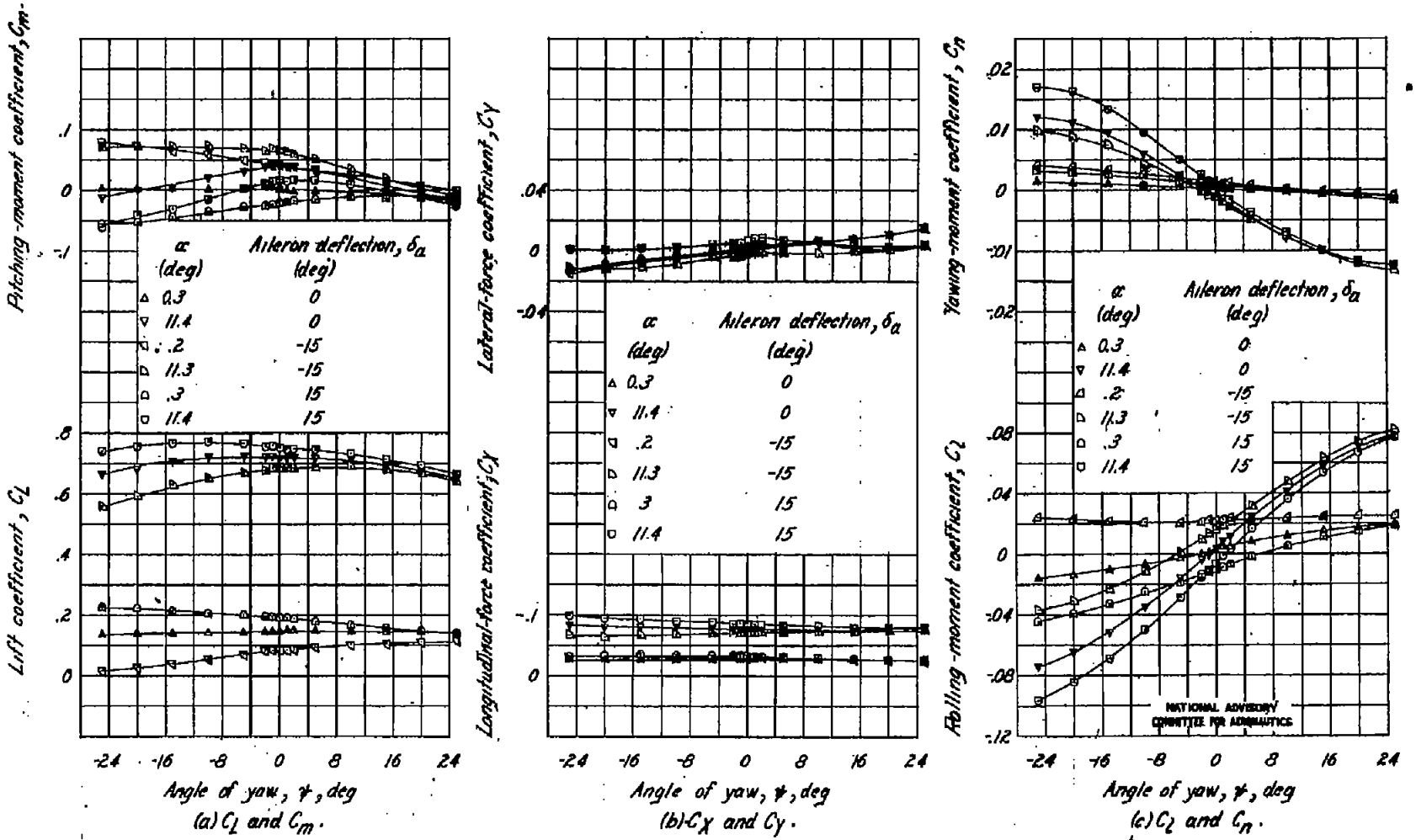

(a) C_L and C_m. (b) C_X and C_Y. (c) C_l and C_n.

Figure 15.-Variation with angle of yaw of the aerodynamic characteristics of a rectangular 45° swept-back wing with a 0.20c chord, 0.50 $\frac{b}{2}$ span aileron on the right wing. A,3.58.

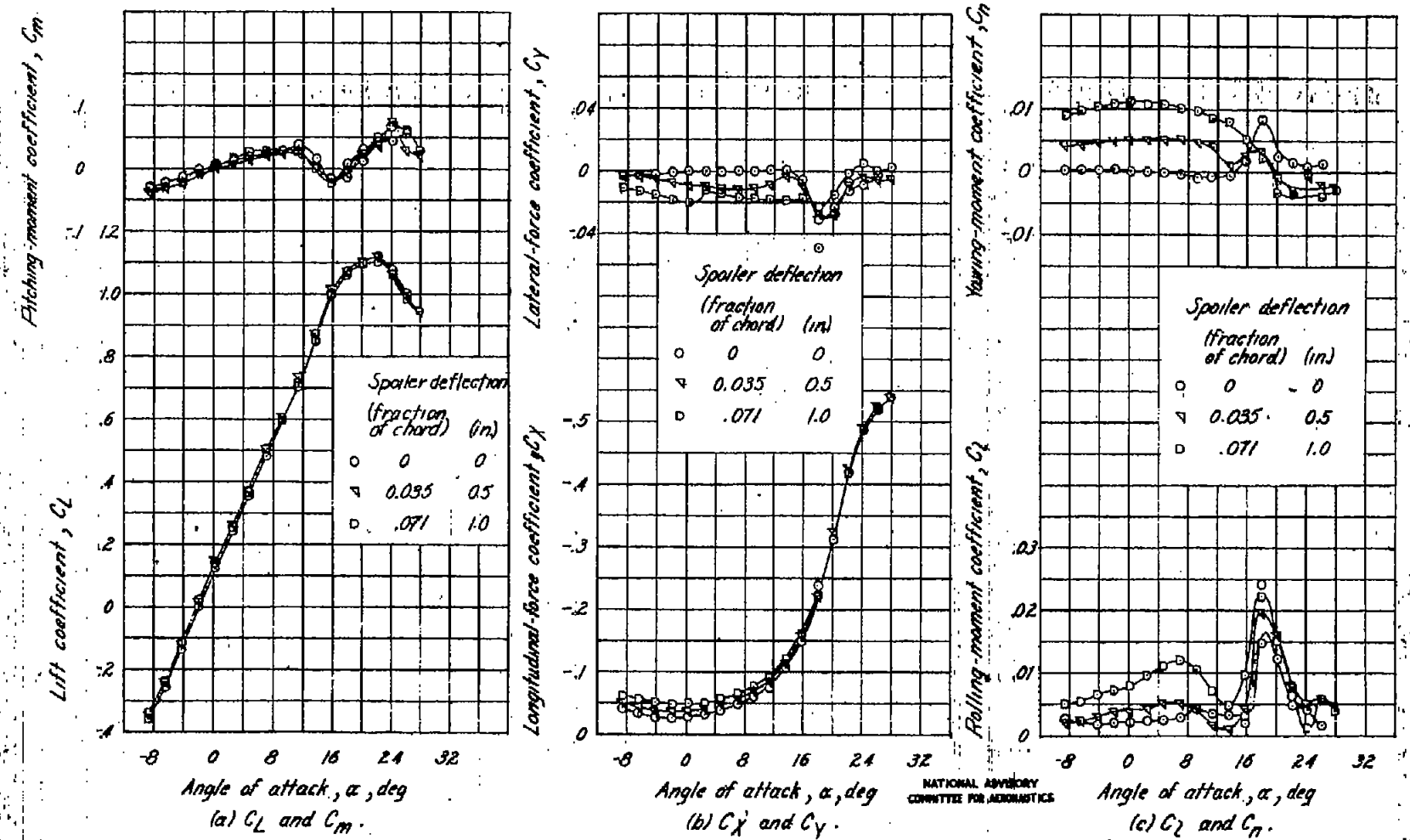

NATIONAL ADVISORY COMMITTEE FOR AERONAUTICS

Figure 16.-Variation with angle of attack of the aerodynamic characteristics of a rectangular 45° swept-back wing with a 0.42 $\frac{b}{2}$ span spoiler on right wing. A, 3.56.

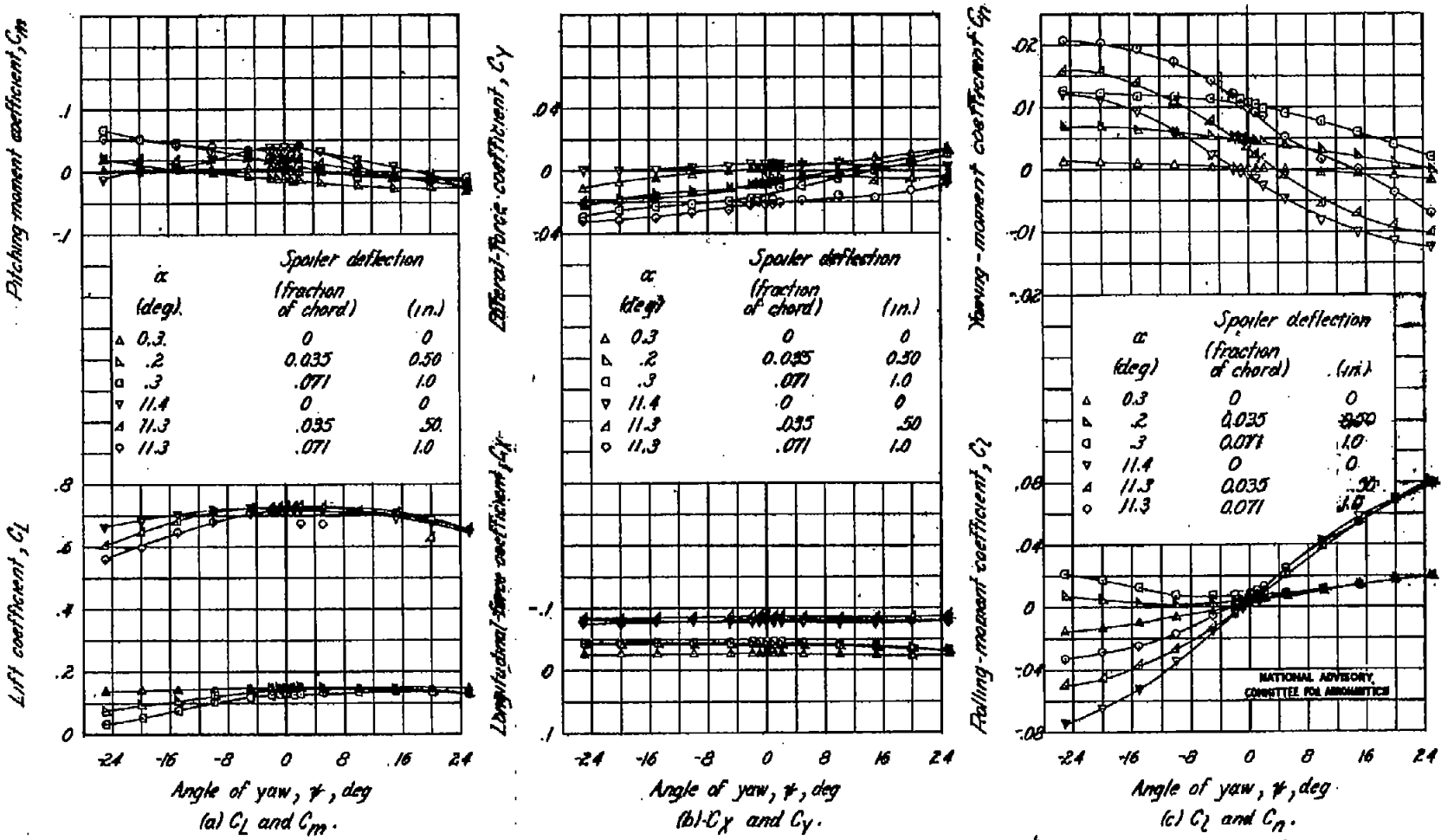

Figure 17.-Variation with angle of yaw of the aerodynamic characteristics of a rectangular 45° swept-back wing with a $0.42\frac{b}{2}$ span spoiler on right wing. A, 3.56.

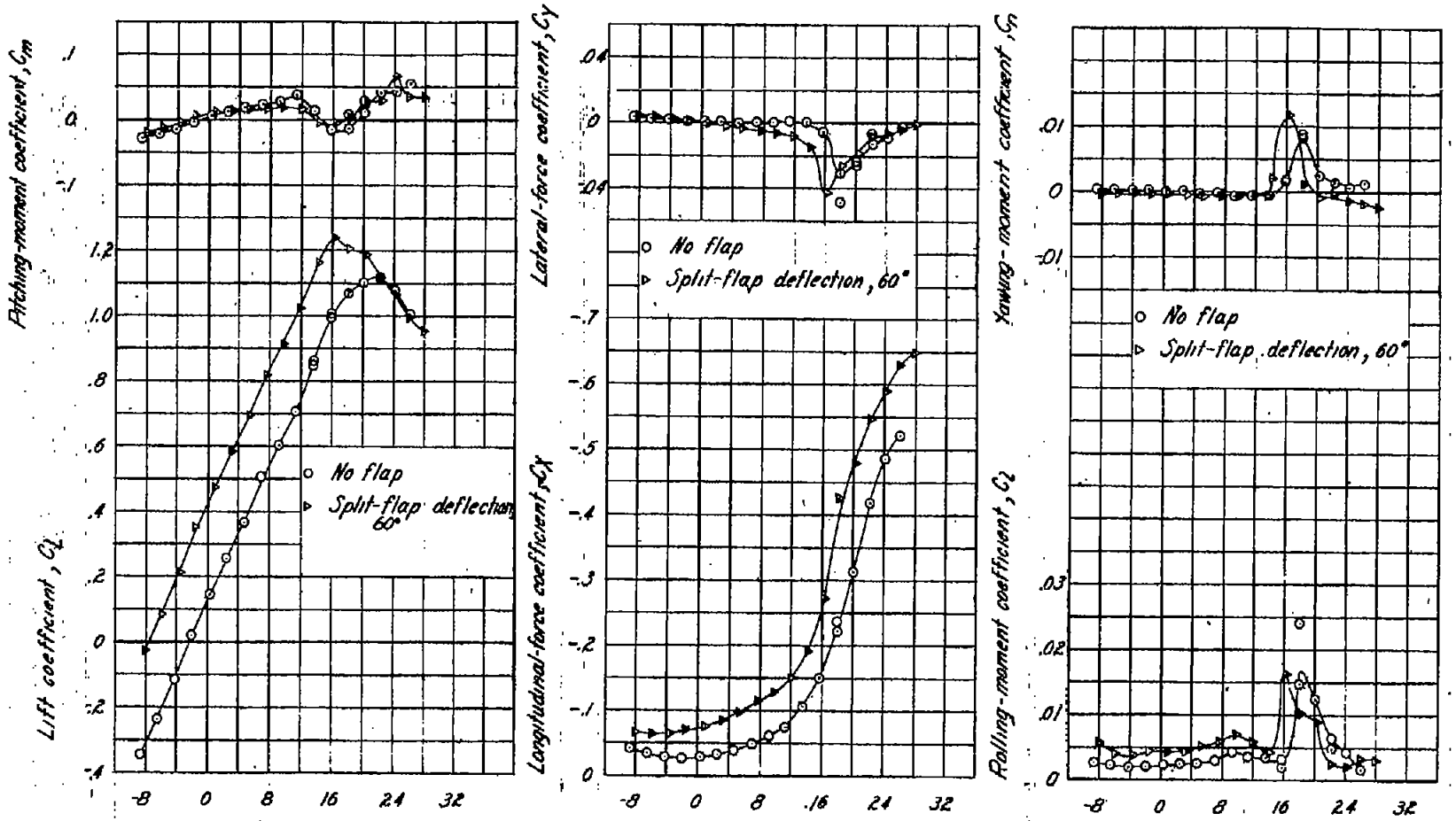

(a) C_L and C_m. (b) C_X and C_Y. (c) C_l and C_n.

NATIONAL ADVISORY COMMITTEE FOR AERONAUTICS

Figure 18.-Variation with angle of attack of the aerodynamic characteristics of a rectangular 45° swept-back wing with a 0.20c chord, 0.50b span split flap deflected 60°. A, 3.56.

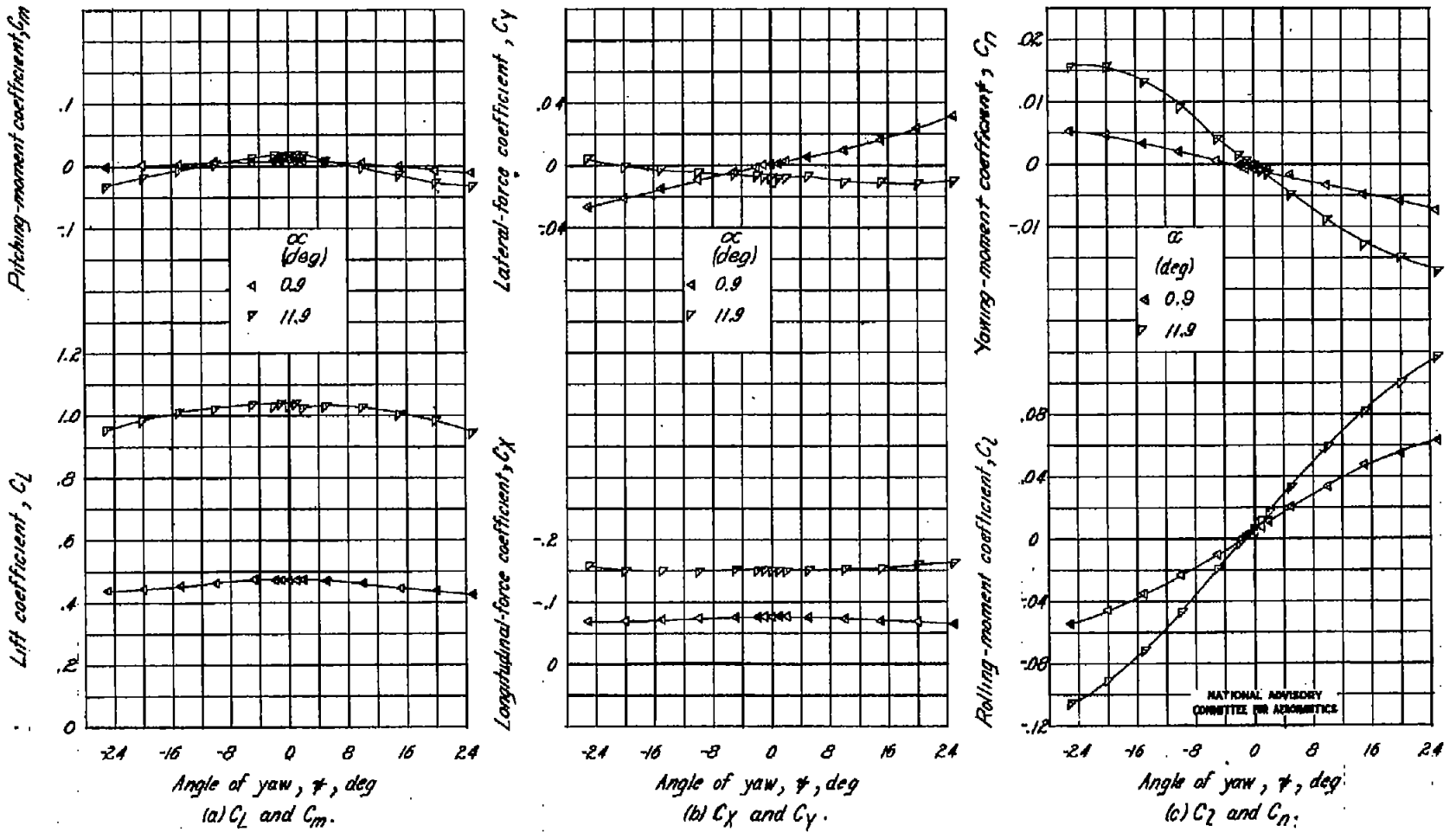

(a) C_L and C_m. (b) C_X and C_Y. (c) C_l and C_n.

Figure 19.-Variation with angle of yaw of the aerodynamic characteristics of a rectangular 45° swept-back wing with a 0.20c chord, 0.50b span split flap deflected 60°. A, 3.56.

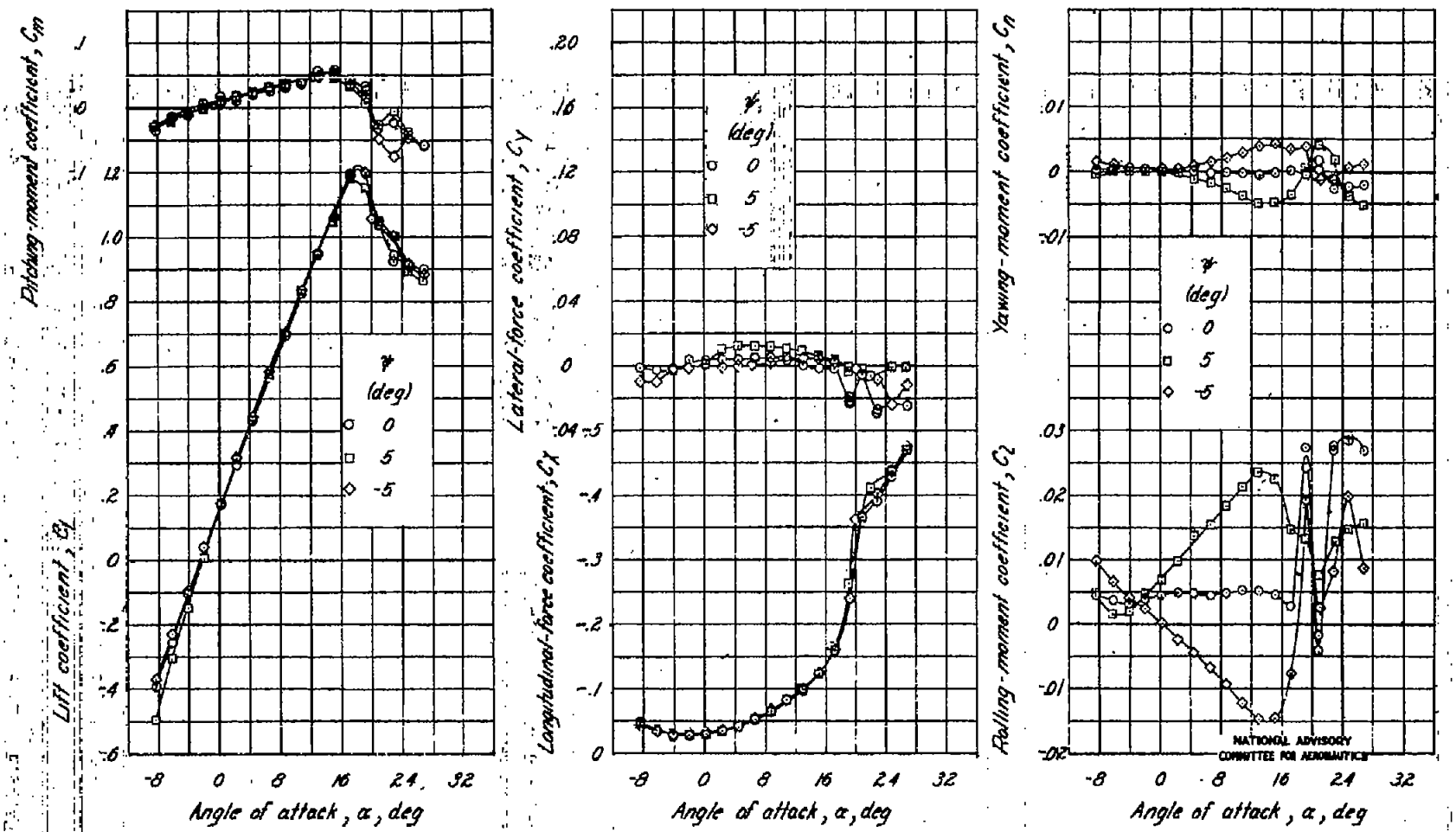

Figure 20.-Variation with angle of attack of the aerodynamic characteristics of a rectangular 30° swept-back wing. A, 4.36.

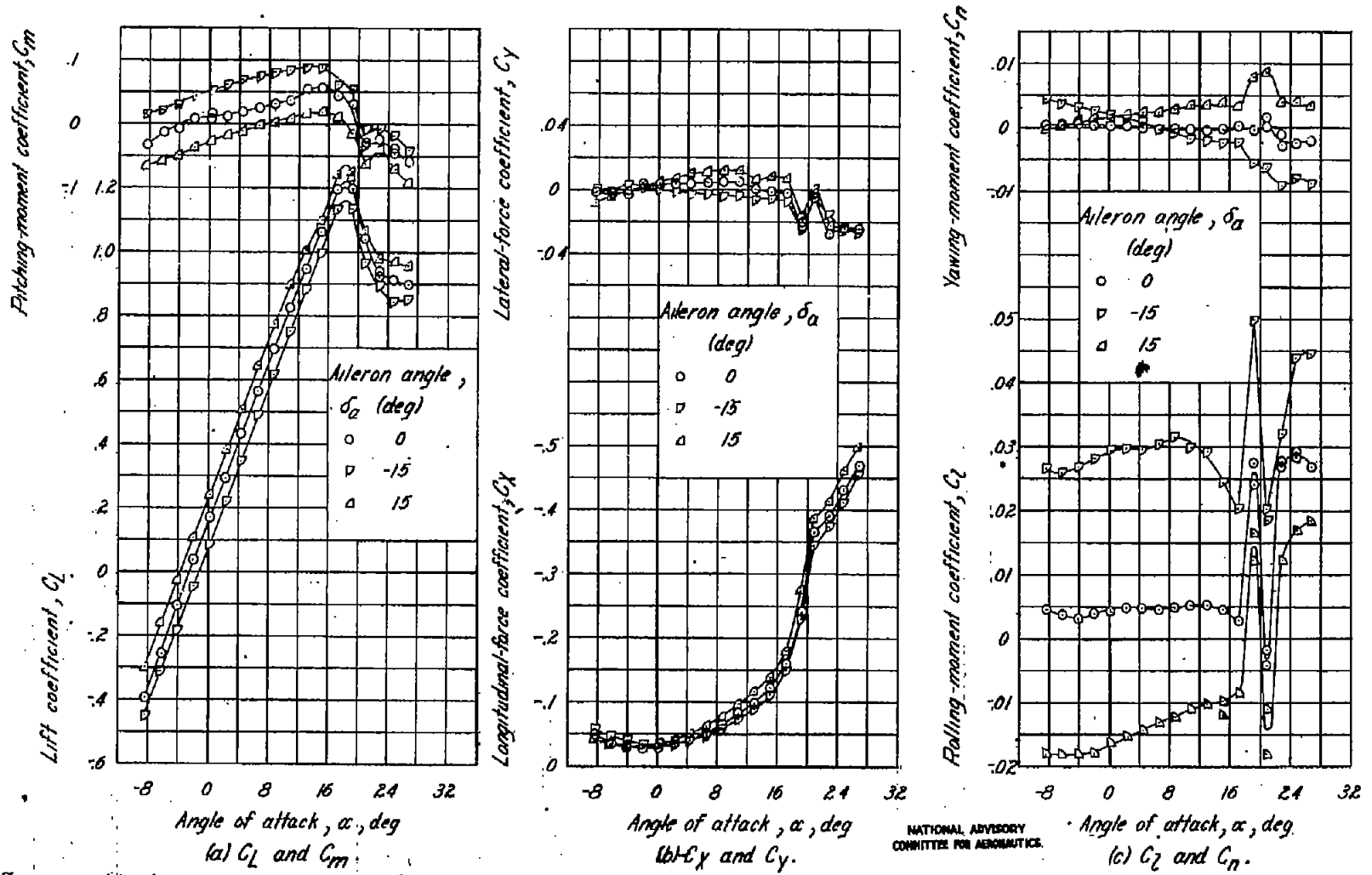

NATIONAL ADVISORY COMMITTEE FOR AERONAUTICS

Figure 21.-Variation with angle of attack of the aerodynamic characteristics of a rectangular 30° swept-back wing with a 0.20c chord, 0.50b/2 span aileron on right wing. A, 4.38.

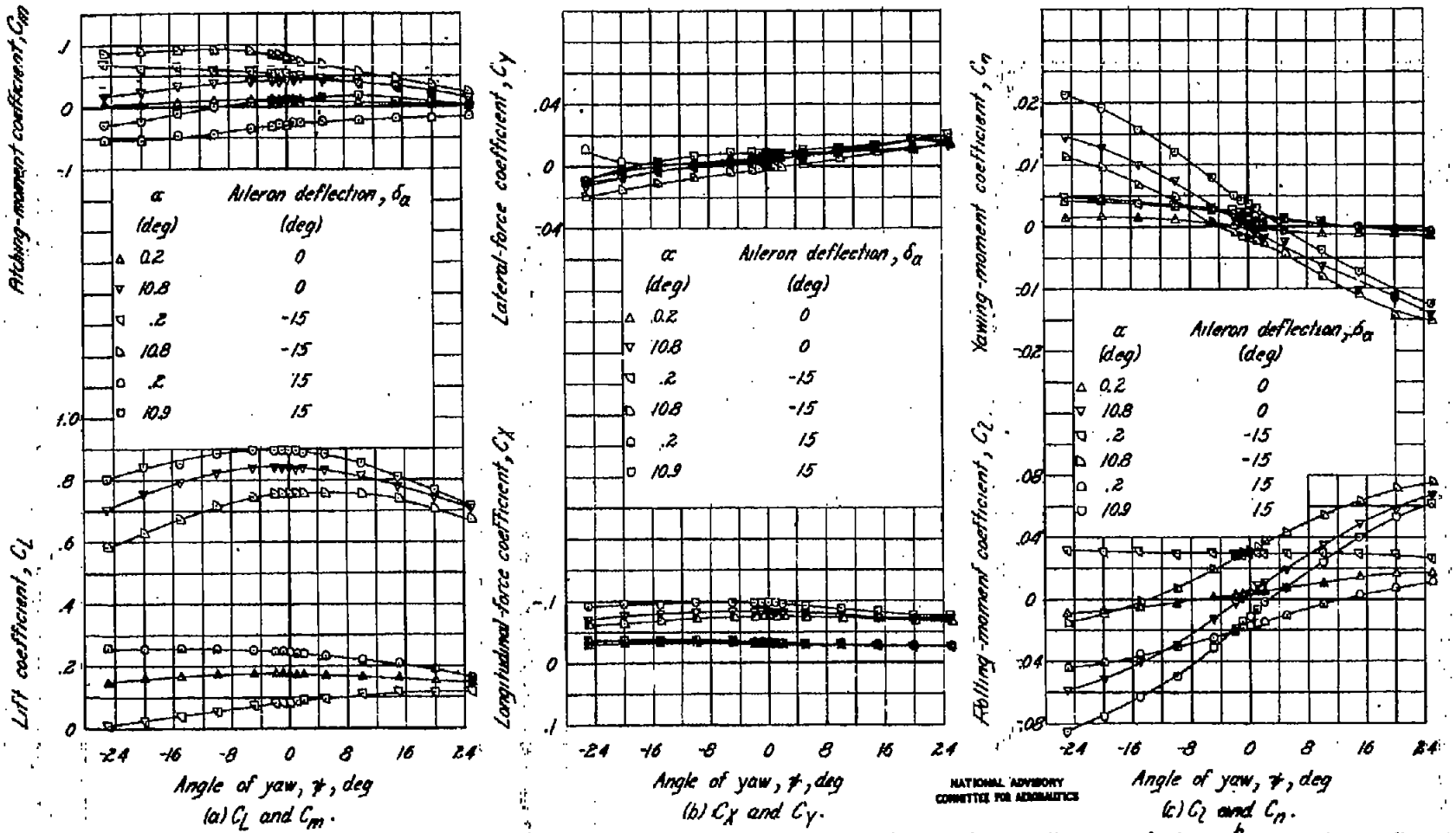

NATIONAL ADVISORY COMMITTEE FOR AERONAUTICS

Figure 22.-Variation with angle of yaw of the aerodynamic characteristics of a rectangular 30° sweptback wing with a 0.20c chord, 0.50 $\frac{b}{2}$ span aileron on the right wing. A, 4.36.

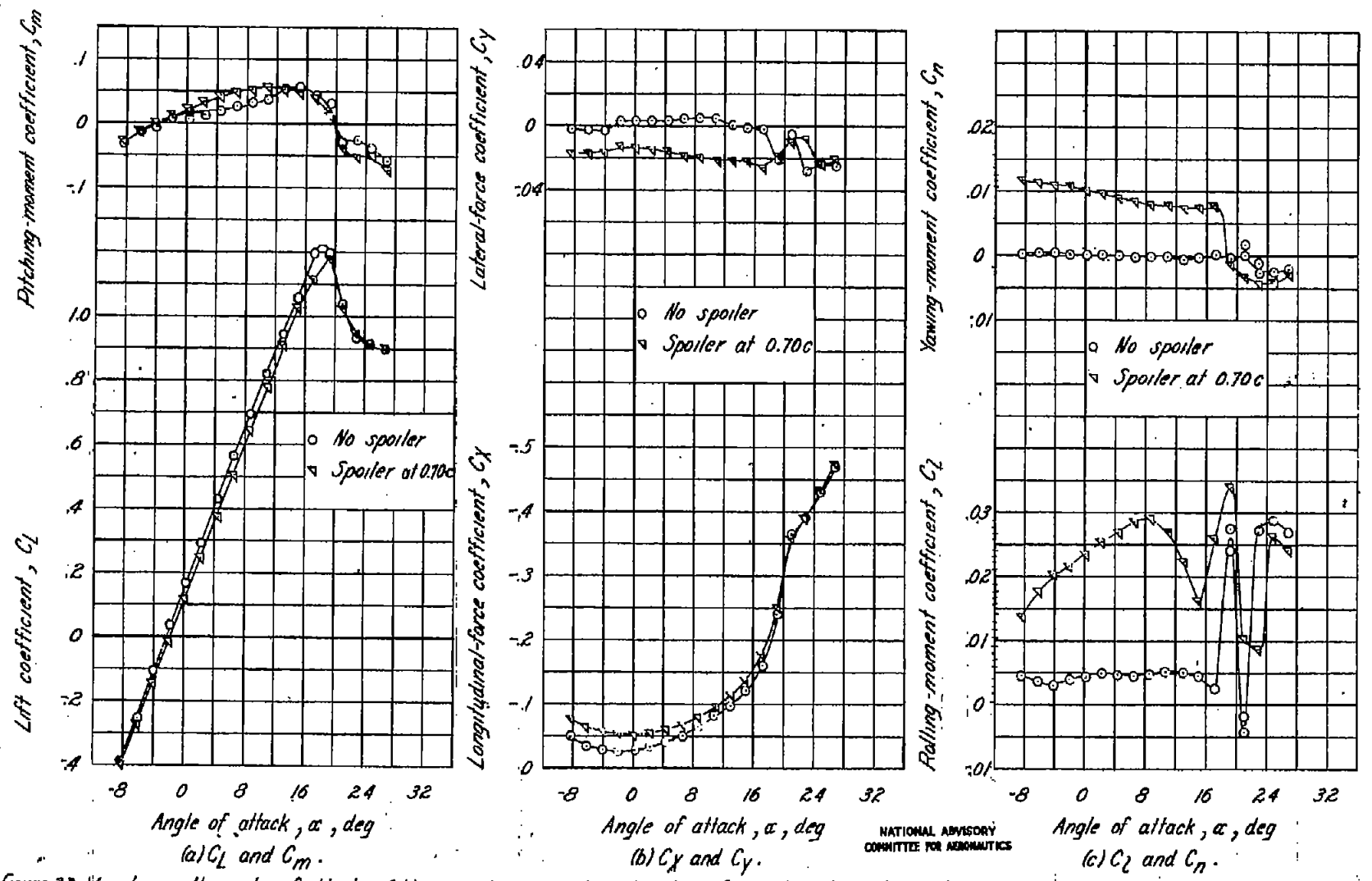

NATIONAL ADVISORY COMMITTEE FOR AERONAUTICS

Figure 23.-Variation with angle of attack of the aerodynamic characteristics of a rectangular 30° sweptback wing with a 0.48 b/2 span spoiler deflected 0.087c on right wing. A 436.

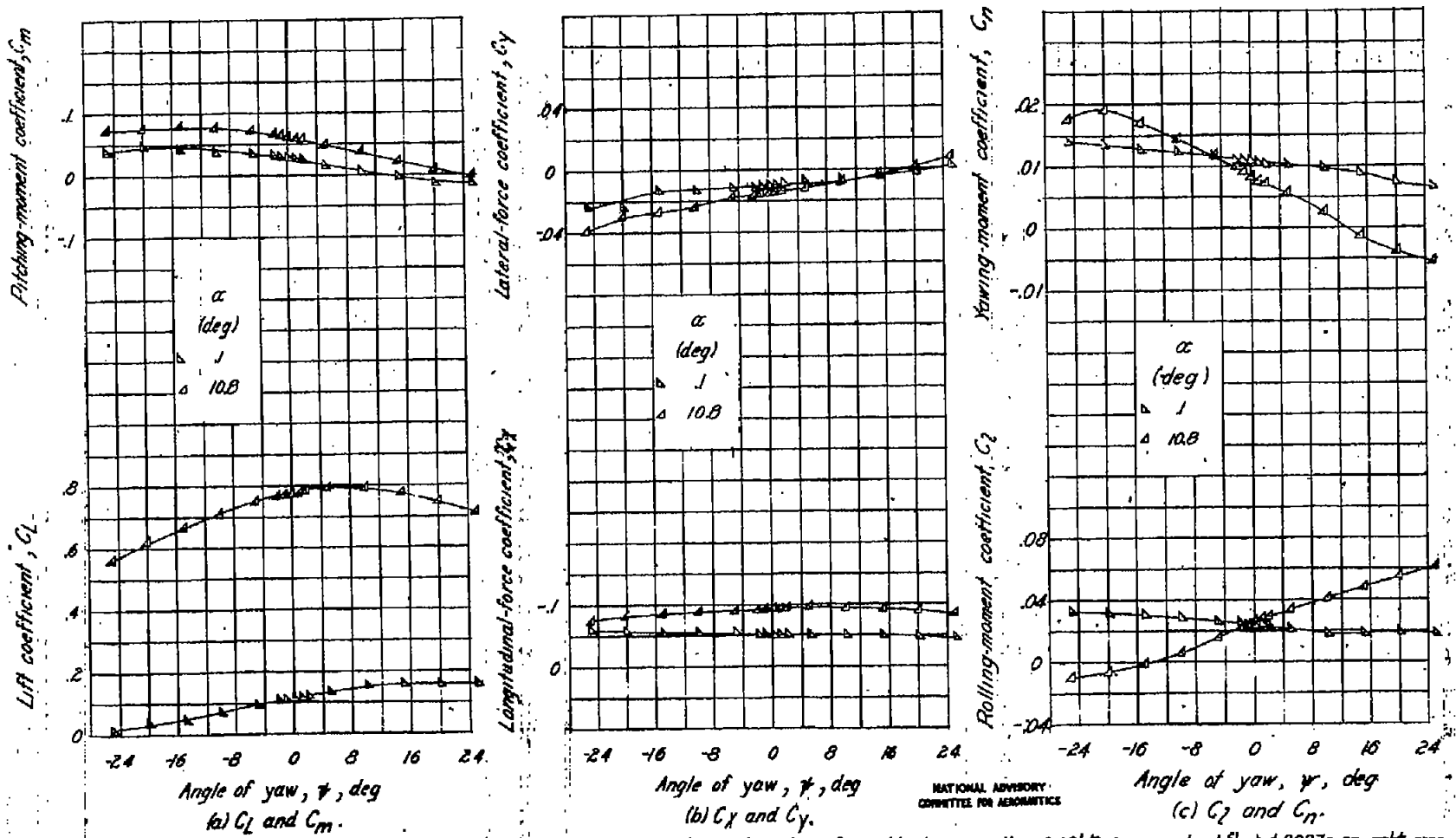

NATIONAL ADVISORY COMMITTEE FOR AERONAUTICS

Figure 24.-Variation with angle of yaw of the aerodynamic characteristics of a rectangular 30° sweep-back wing with a 0.46b/2 span spoiler deflected 0.087c on right wing. A, 4.36.

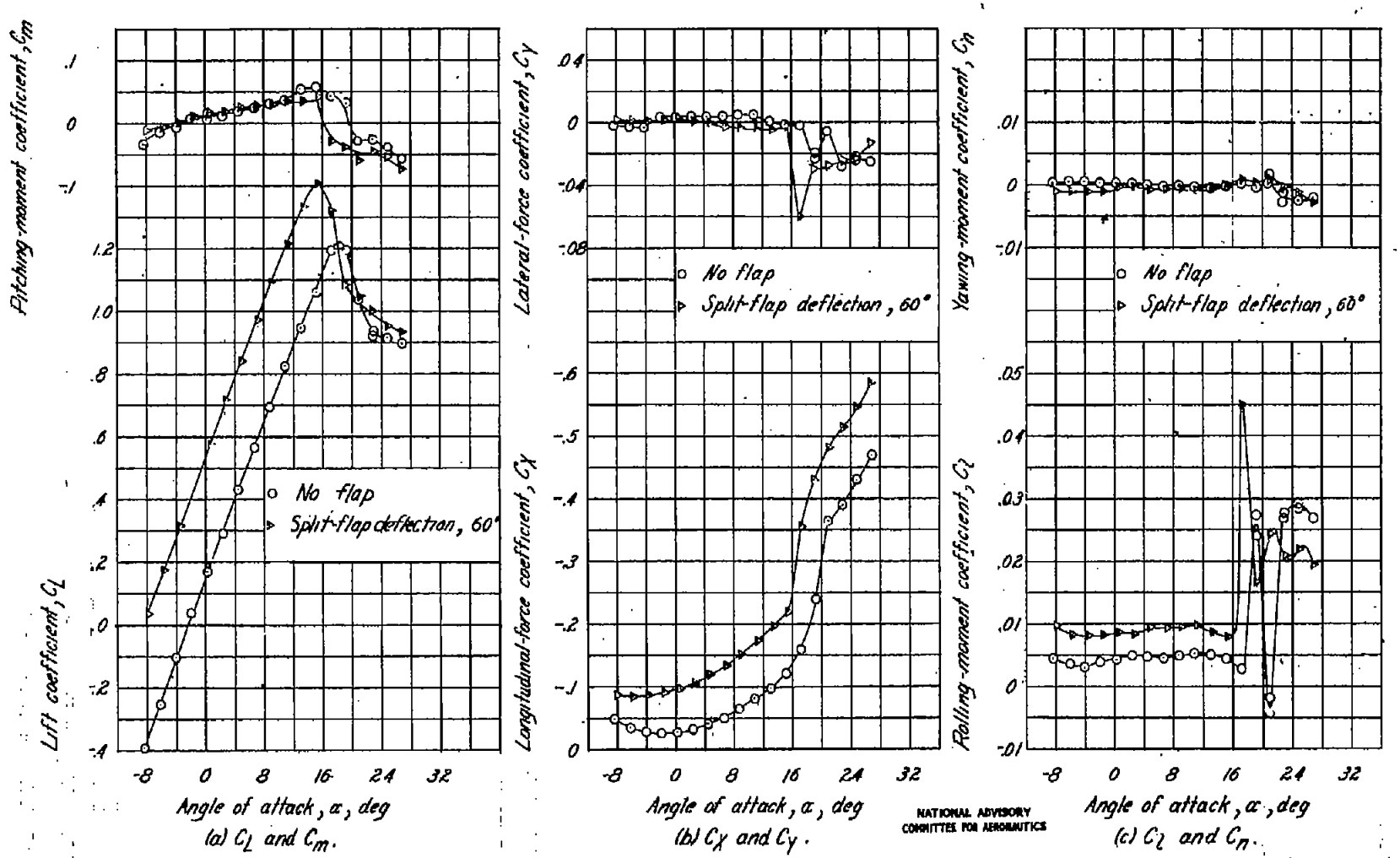

NATIONAL ADVISORY COMMITTEE FOR AERONAUTICS

Figure 25.-Variation with angle of attack of the aerodynamic characteristics of a rectangular 30° swept-back wing with a 0.20c chord 0.50b span split flap deflected 60°. A, 4.36.

Fig. 26a-C_L

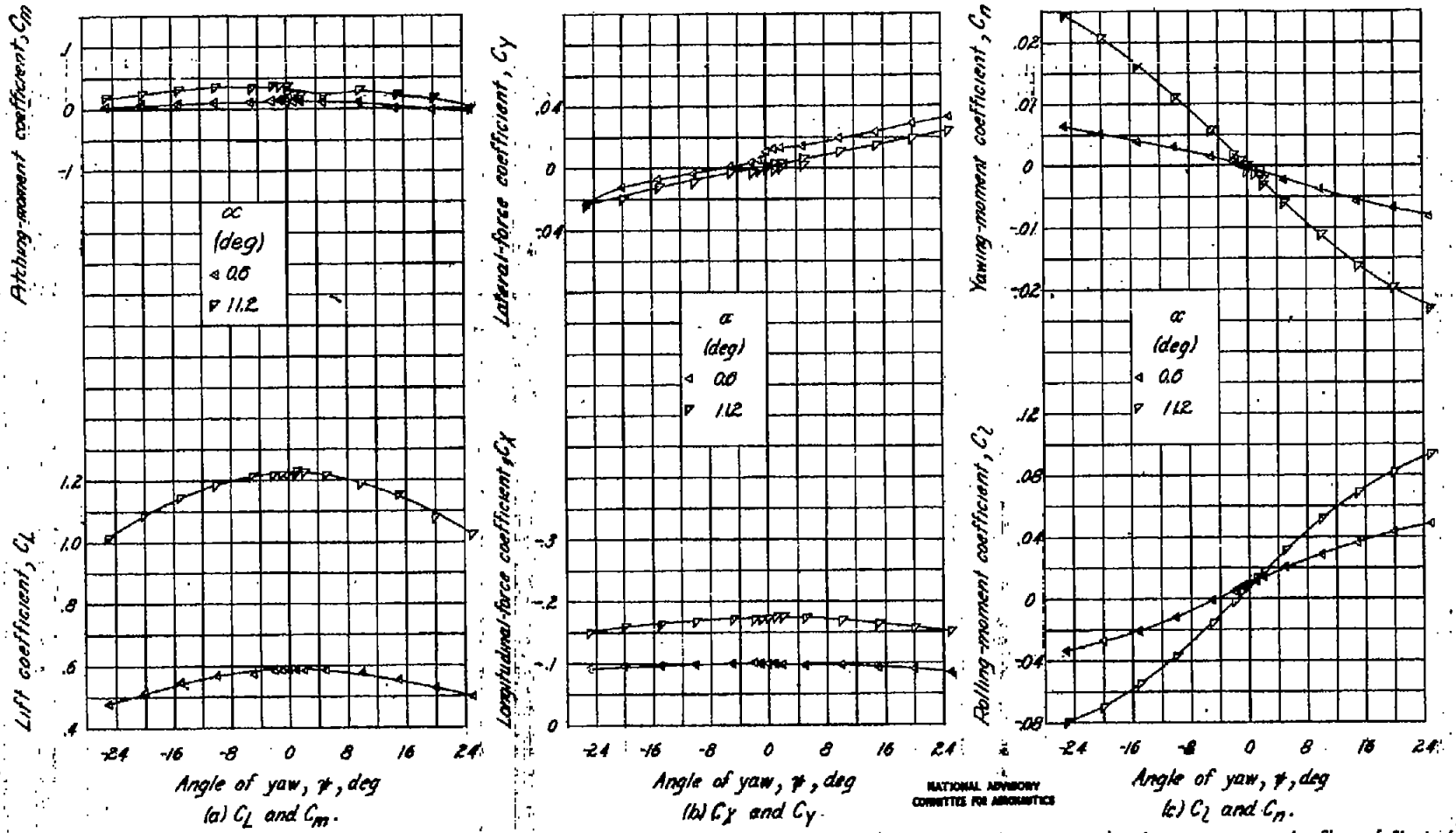

NATIONAL ADVISORY COMMITTEE FOR AERONAUTICS

Figure 26.-Variation with angle of yaw of the aerodynamic characteristics of a rectangular 30° swept-back wing with a 0.20c chord, 0.50b span split flap, deflected 60°. A, 4.36.

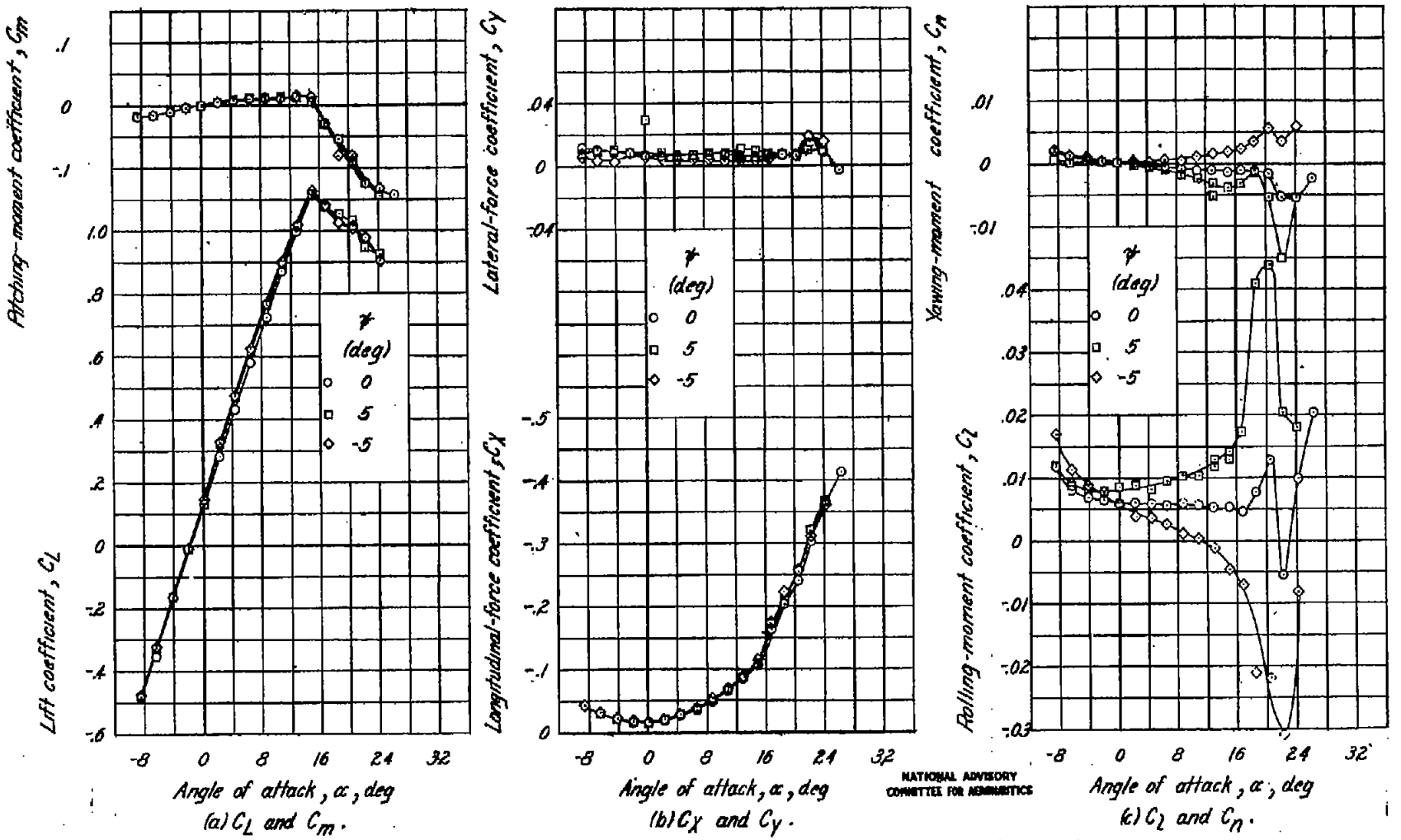

Figure 27.-Variation with angle of attack of the aerodynamic characteristics of a rectangular 0° swept-back wing. A, 5.03.

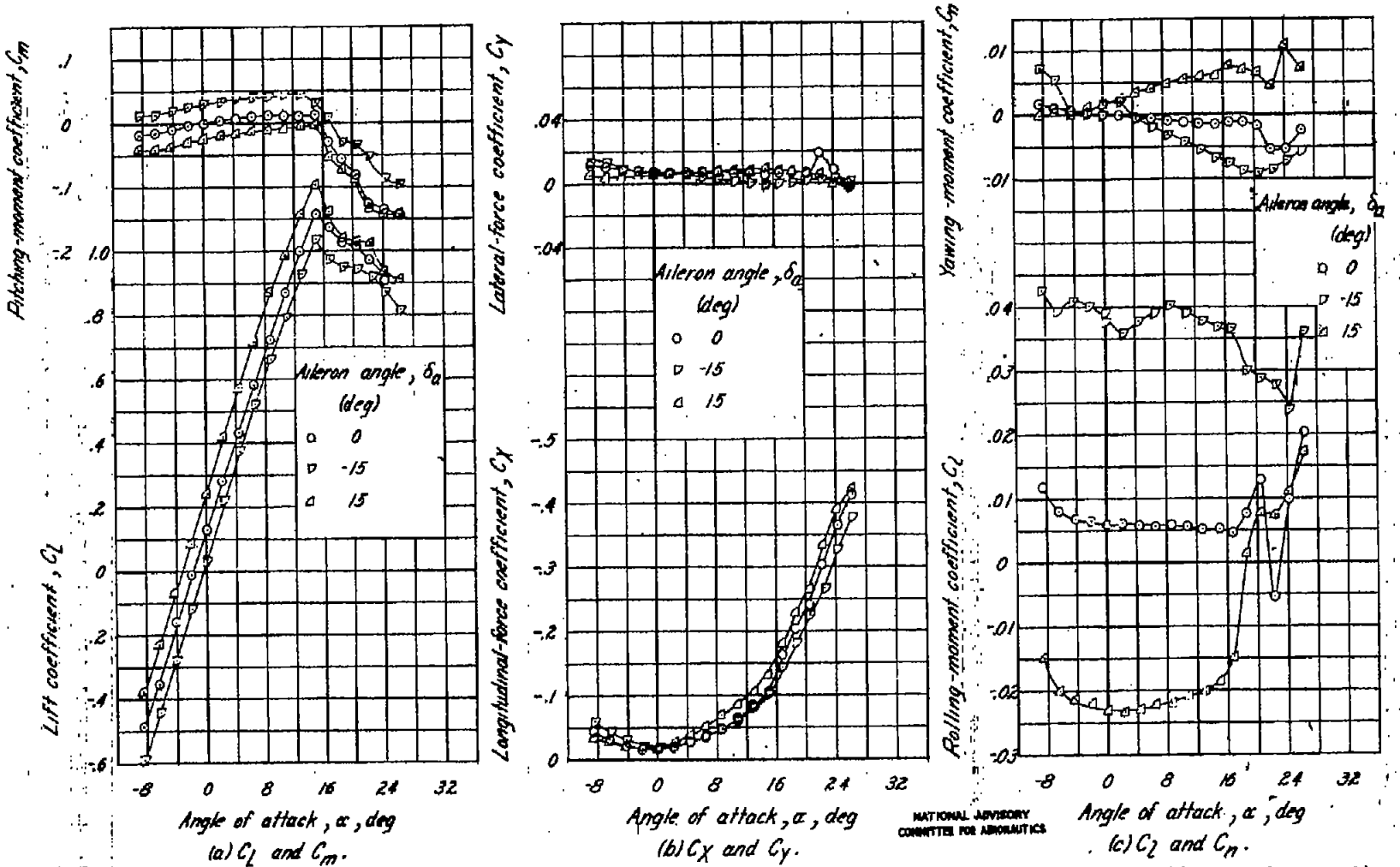

NATIONAL ADVISORY COMMITTEE FOR AERONAUTICS

Figure 28.-Variation with angle of attack of the aerodynamic characteristics of a rectangular 0° swept-back wing with a 0.20c chord, 0.50b/2 span aileron on right wing. A, 5.03.

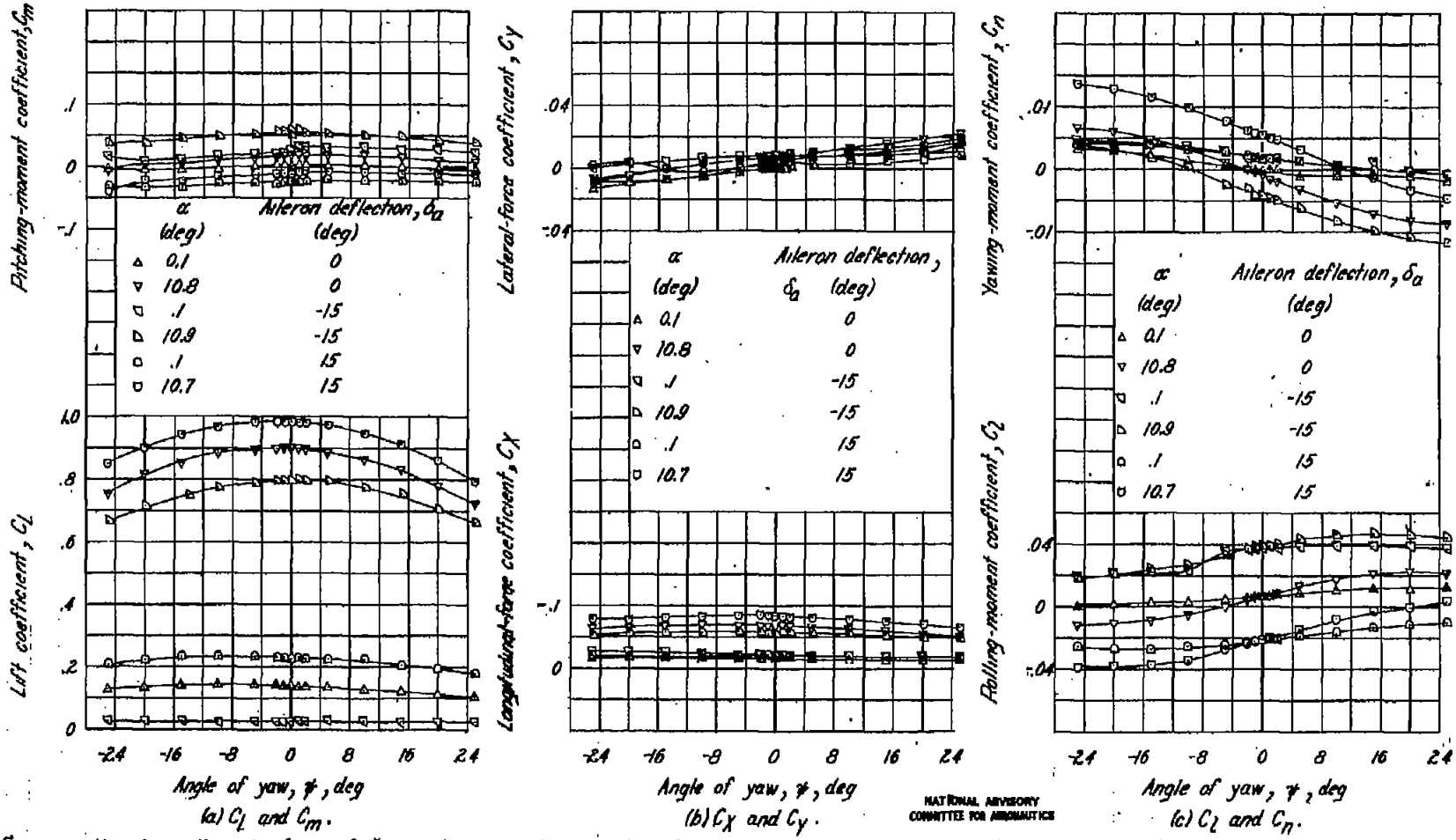

NATIONAL ADVISORY COMMITTEE FOR AERONAUTICS

Figure 29a.-Variation with angle of yaw of the aerodynamic characteristics of a rectangular 0° sweptback wing with a 0.20c chord, 0.50b/2 span aileron on the right wing. A, 5.03.

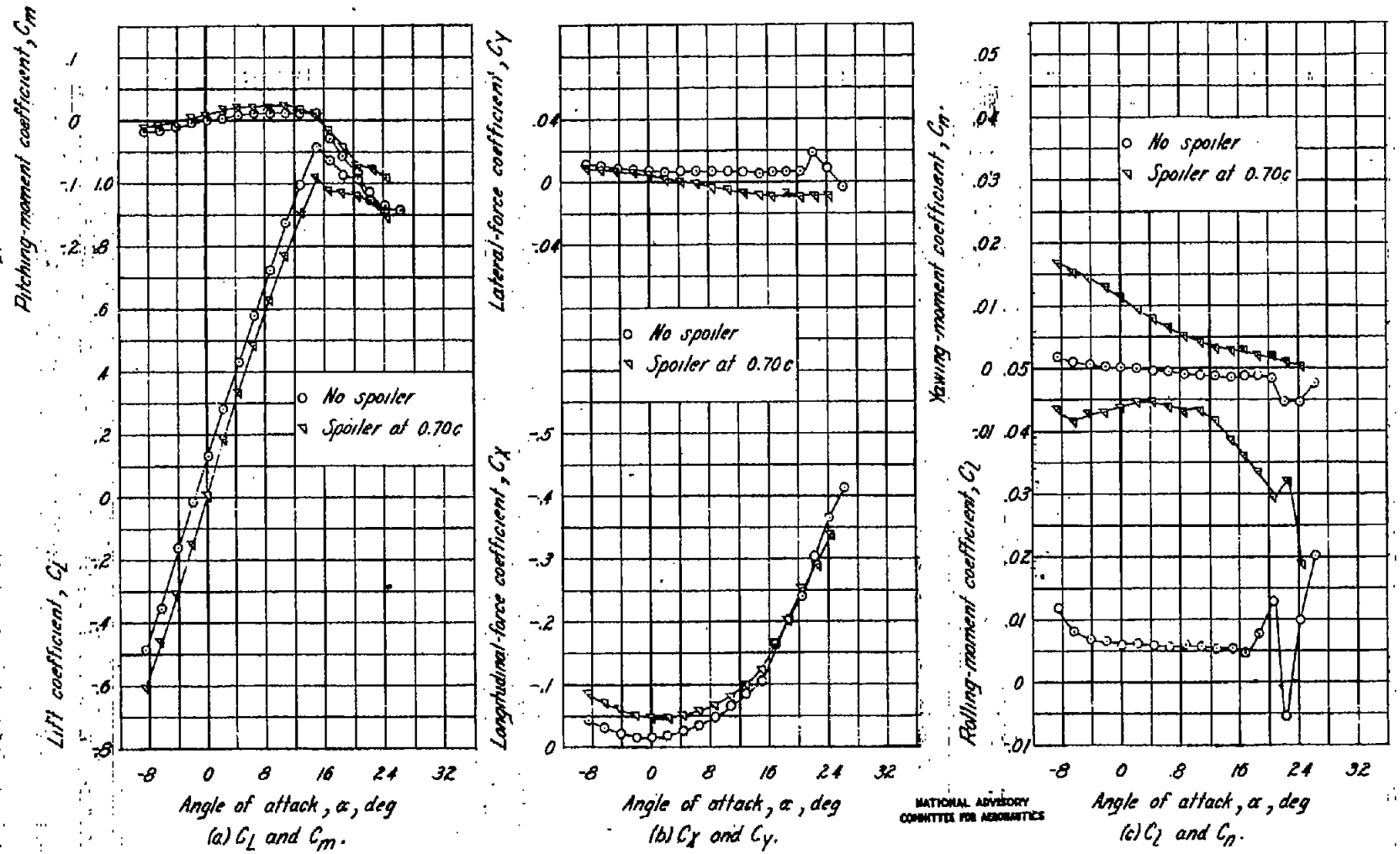

NATIONAL ADVISORY COMMITTEE FOR AERONAUTICS

Figure 30.-Variation with angle of attack of the aerodynamic characteristics of a rectangular 0° sweptback wing with a 0.50 b/2 span spoiler deflected 0.10c on right wing. A,503.

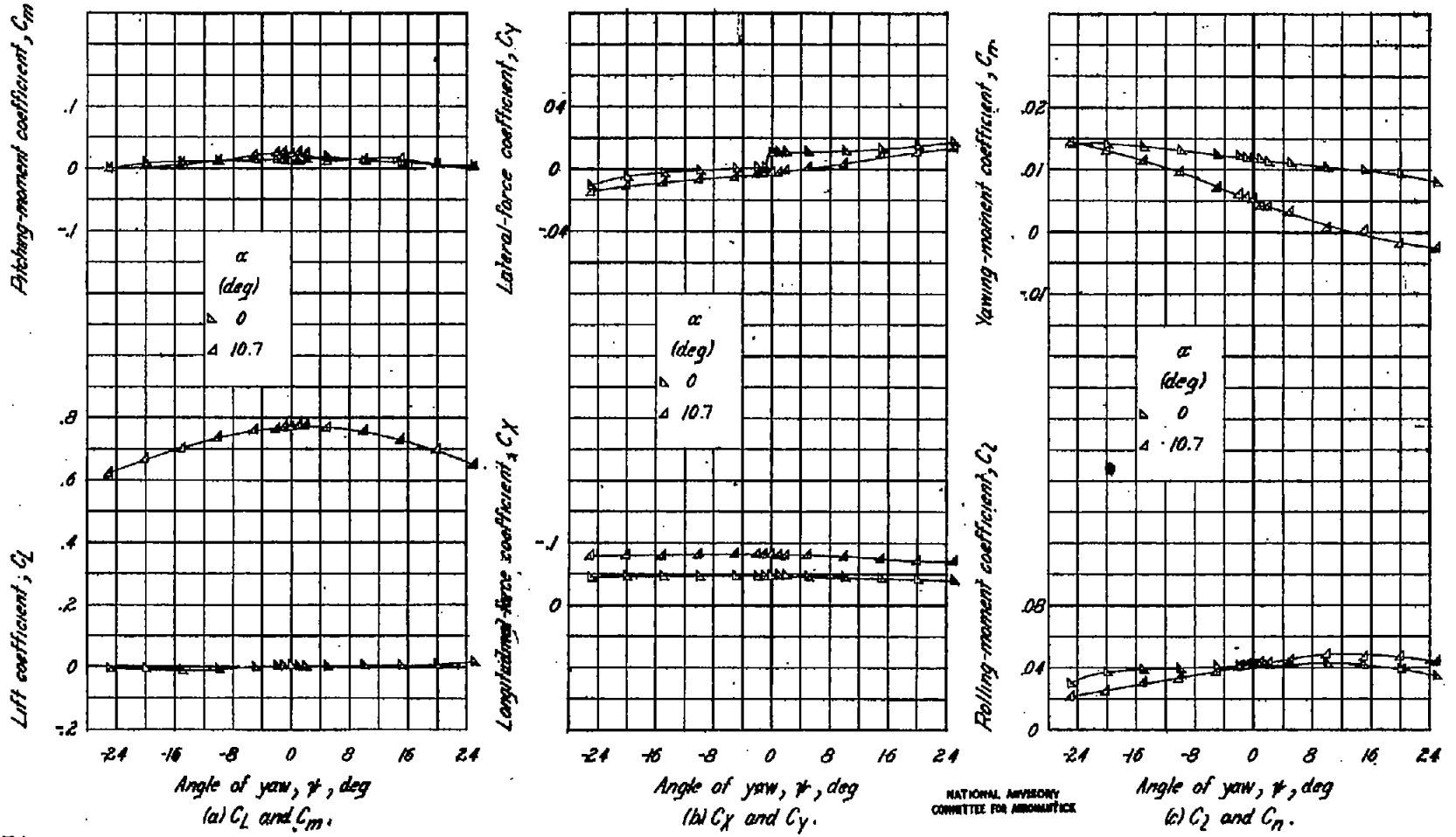

NATIONAL ADVISORY COMMITTEE FOR AERONAUTICS

Figure 31.-Variation with angle of yaw of the aerodynamic characteristics of a rectangular 0° sweptback wing with a 0.50 b/2 span spoiler deflected 0.10 c on right wing. A, 5.03.

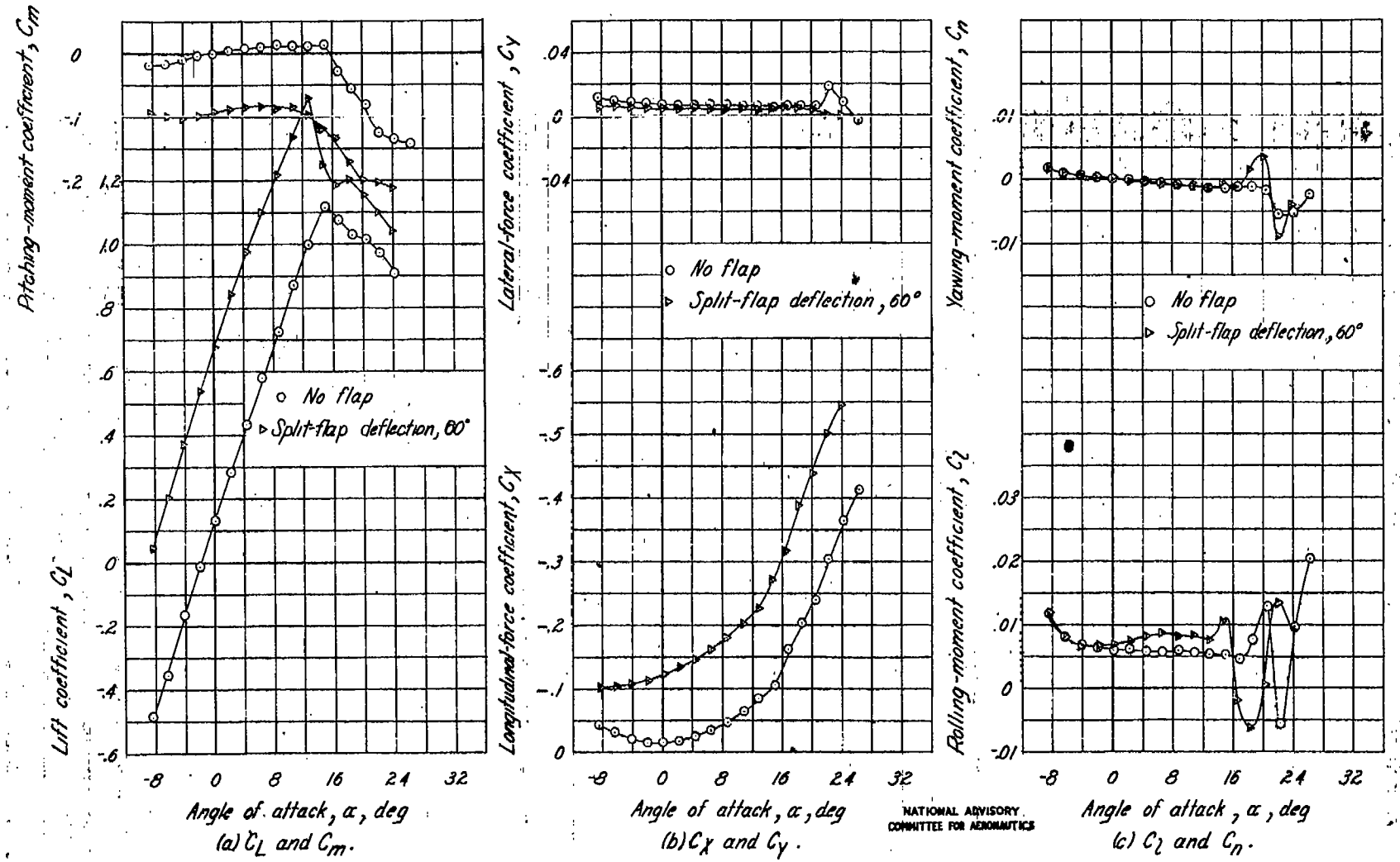

NATIONAL ADVISORY COMMITTEE FOR AERONAUTICS

Figure 32.-Variation with angle of attack of the aerodynamic characteristics of a rectangular 0° swept-back wing with a 0.20c chord, 0.50b span split flap deflected 60°: A, 5.03.

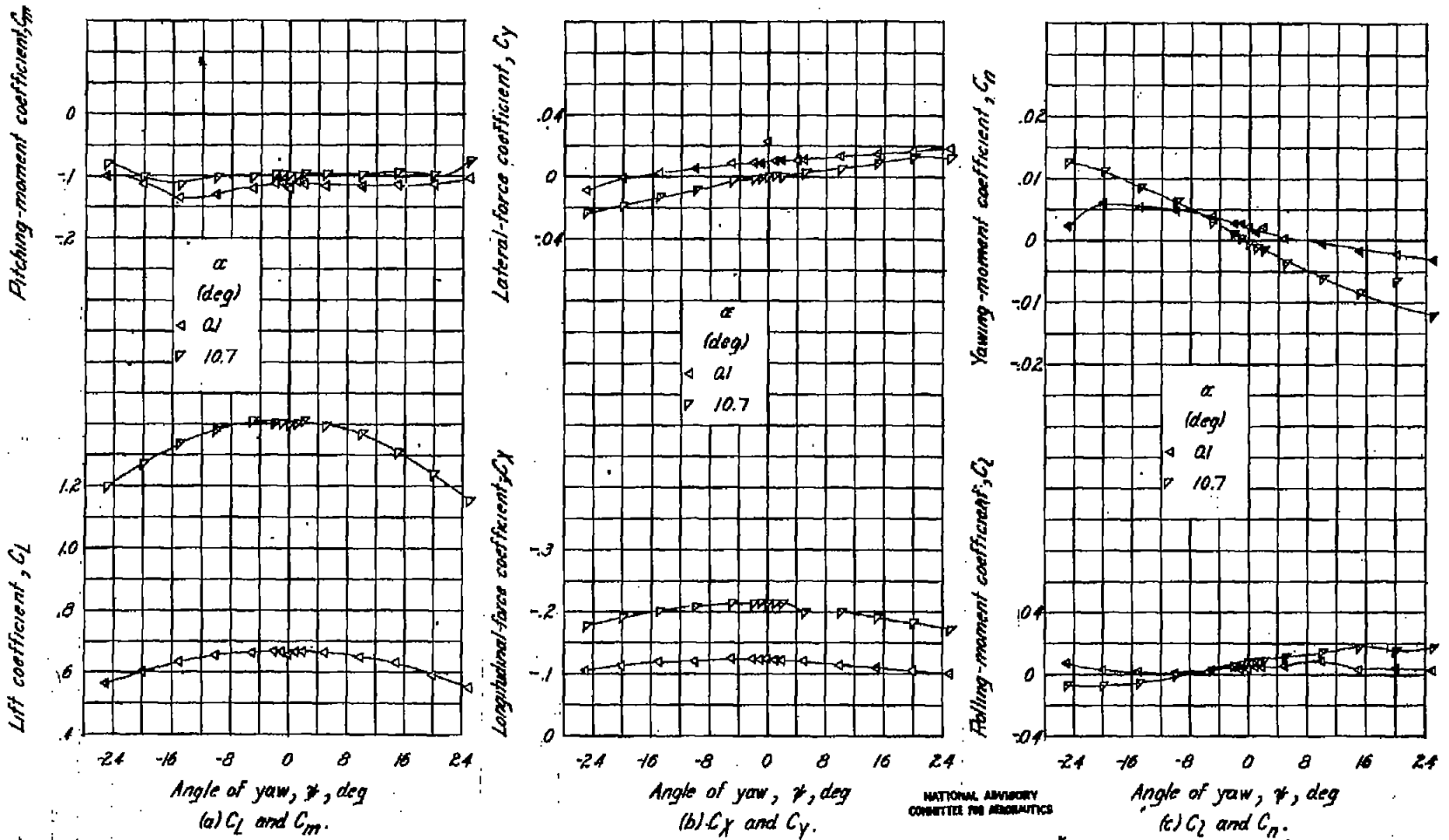

Figure 33.-Variation with angle of yaw of the aerodynamic characteristics of a rectangular 0° swept-back wing with a 0.20c chord, 0.50b span split flap deflected 60°. A, 5.03.

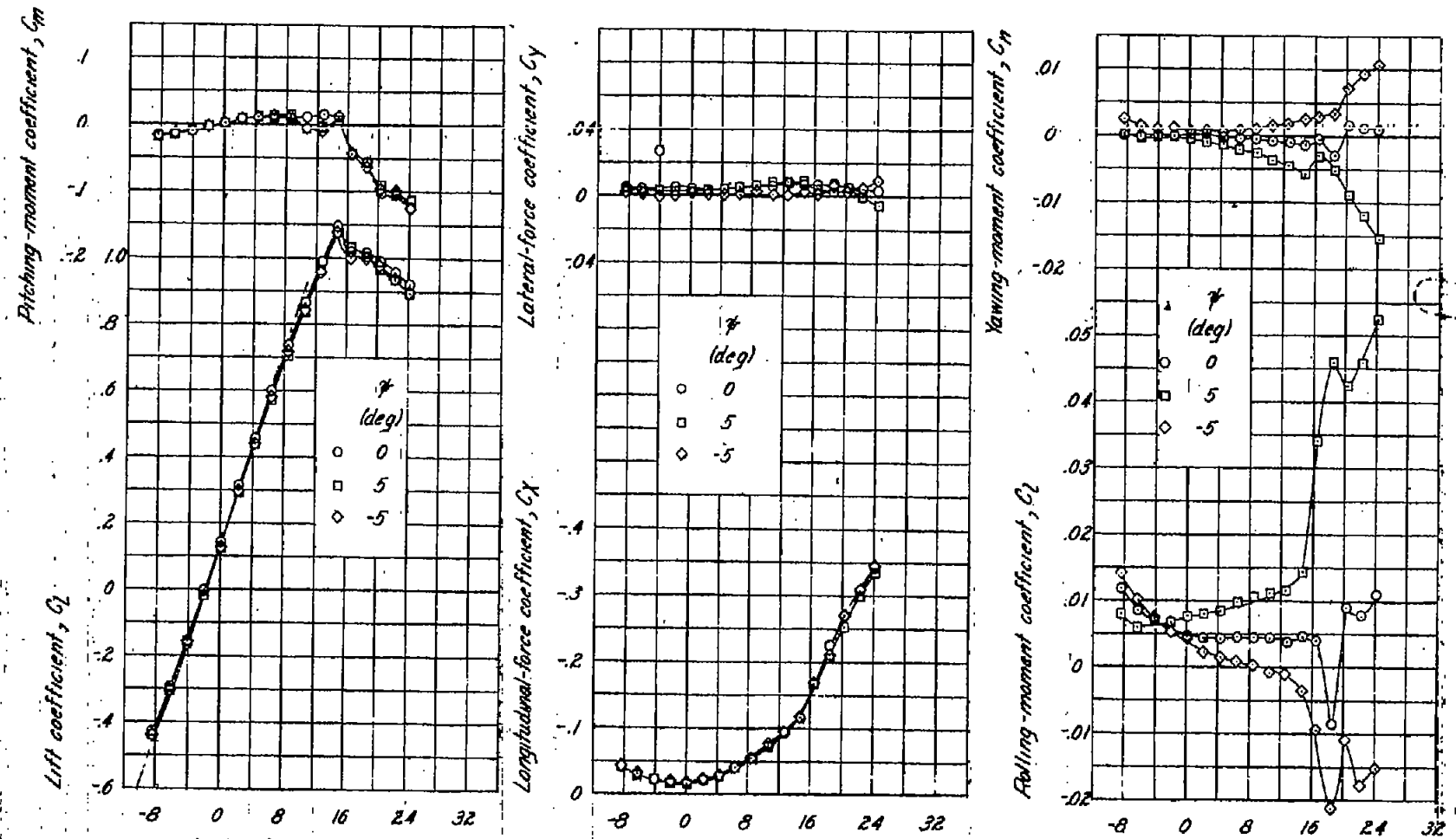

NATIONAL ADVISORY COMMITTEE FOR AERONAUTICS

Figure 34.-Variation with angle of attack of the aerodynamic characteristics of a rectangular 0° swept-back wing. A, 4.13.

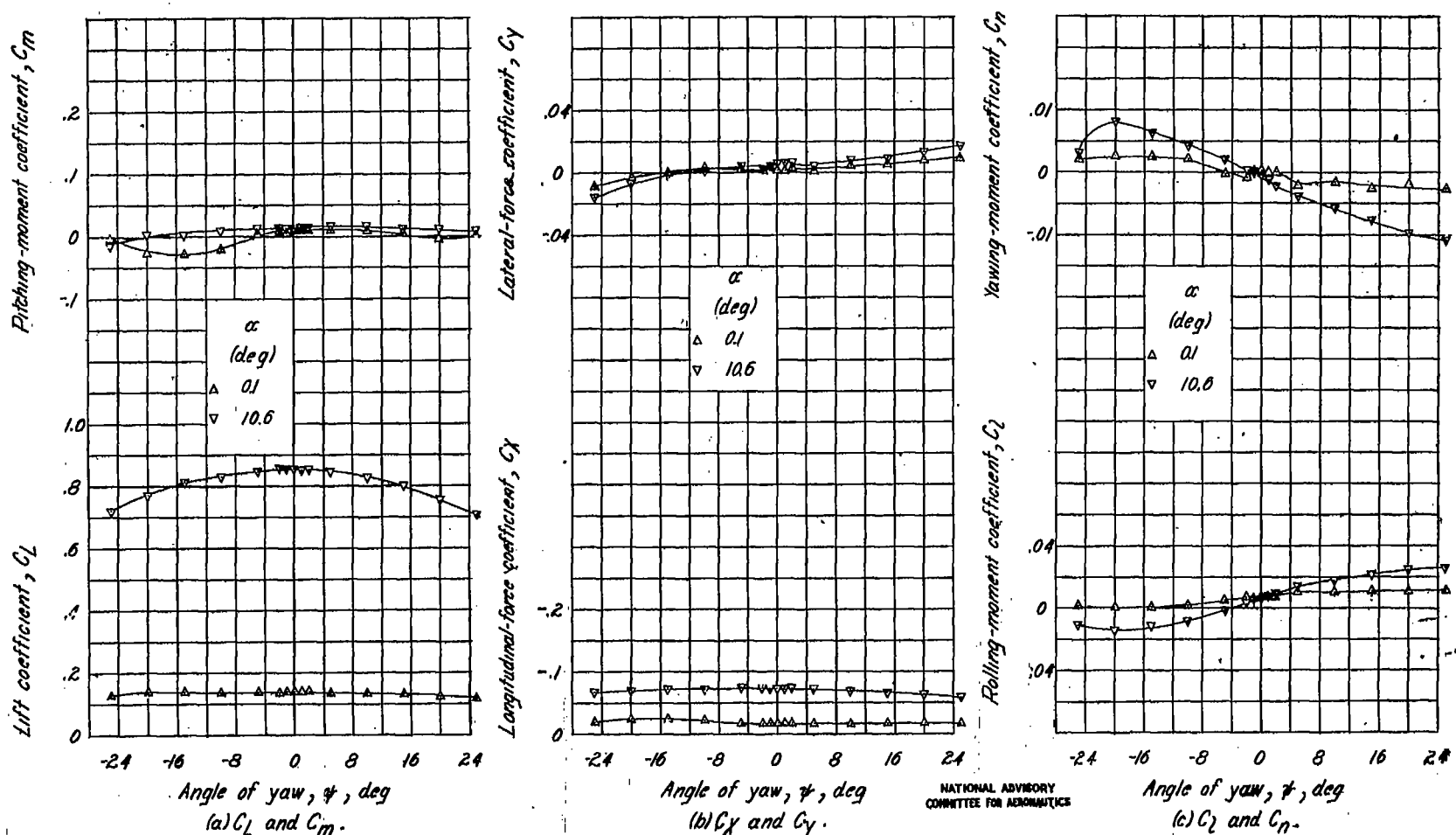

Figure 35.-Variation with angle of yaw of the aerodynamic characteristics of a rectangular 0° swept-back wing. A, 4.13.

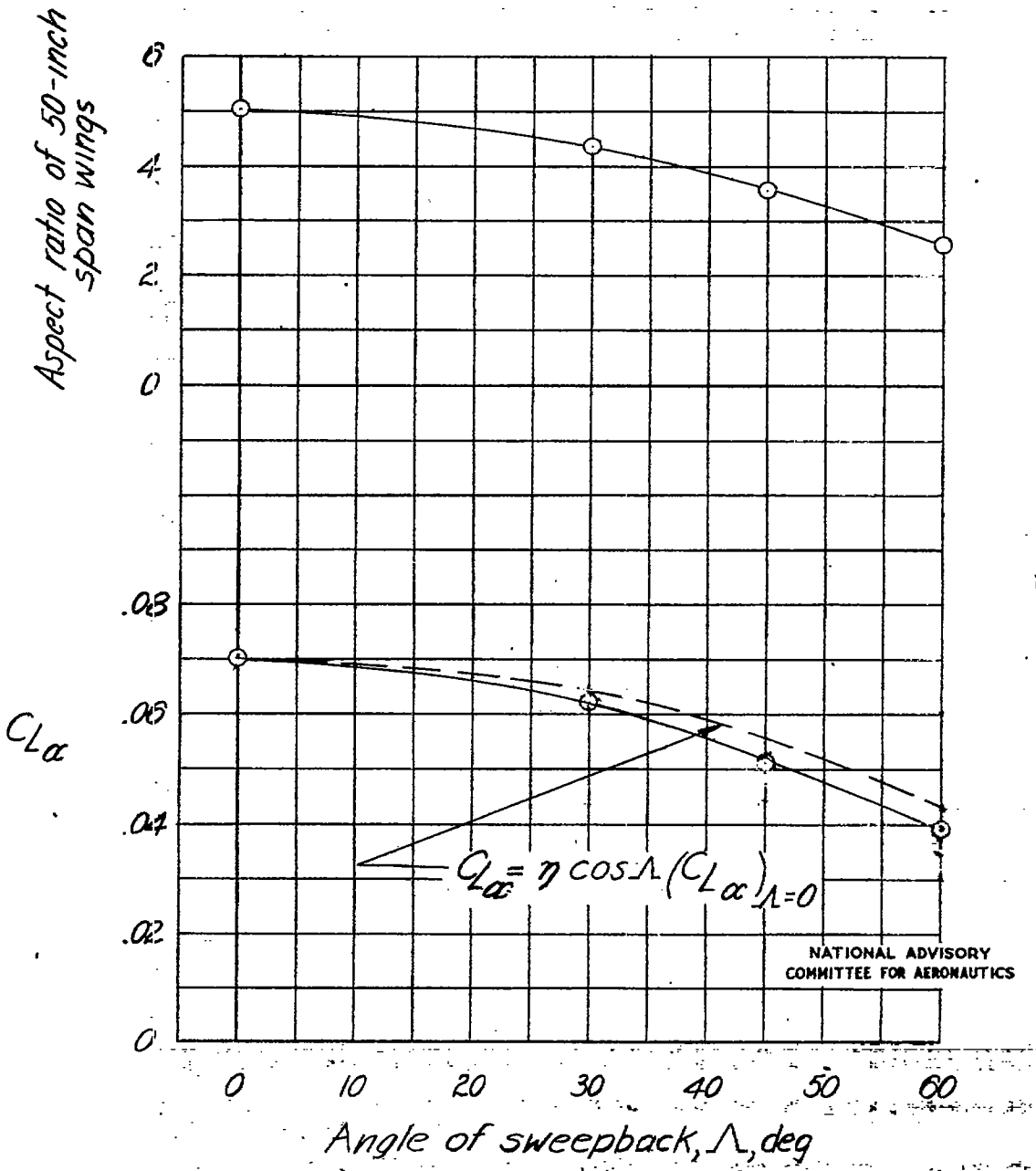

Figure 36.- Variation with sweepback of aspect ratio and of the estimated and experimental values of C_{L_α}.

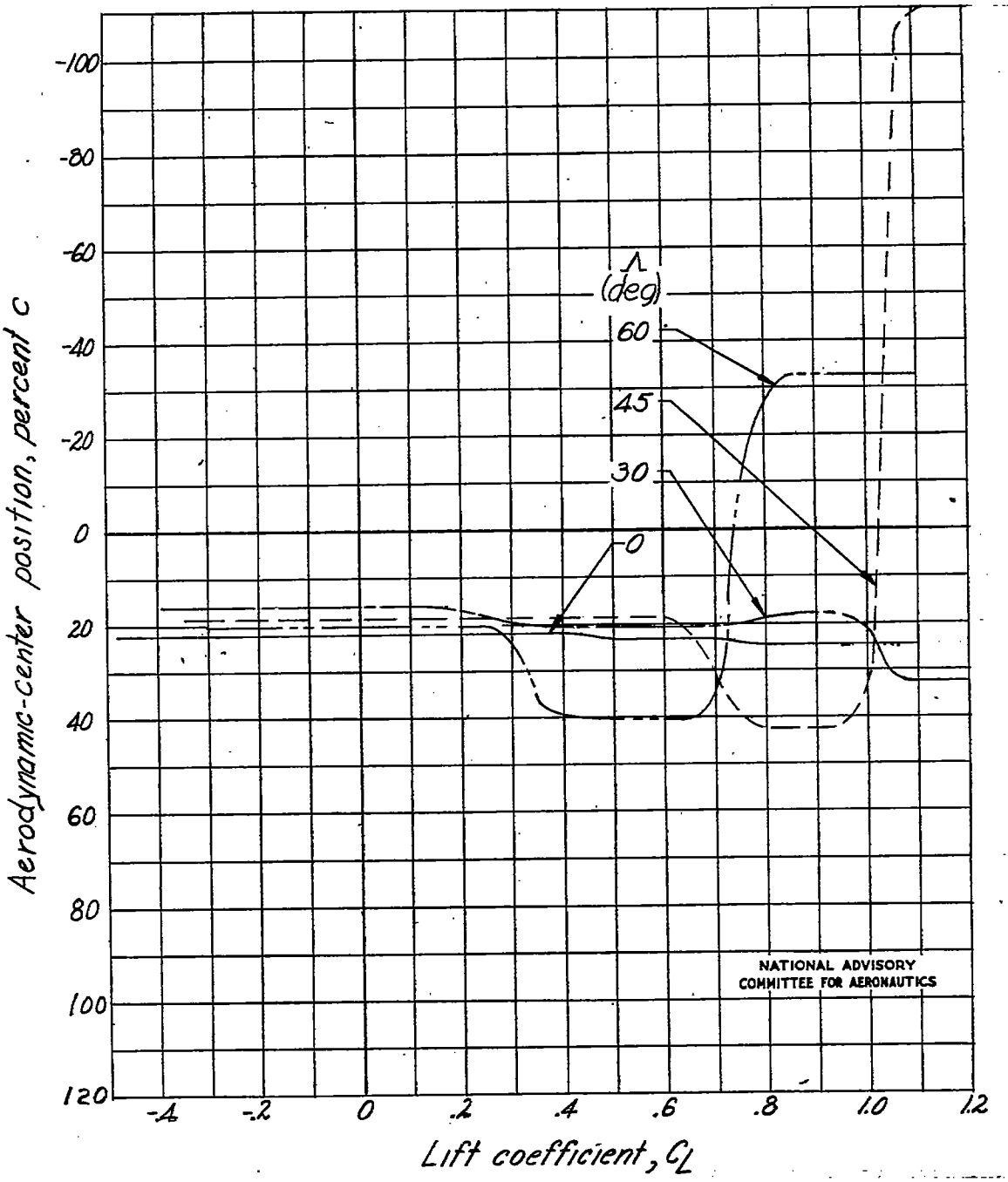

Figure 37.- Variation of aerodynamic-center position with lift coefficient for several angles of sweepback.

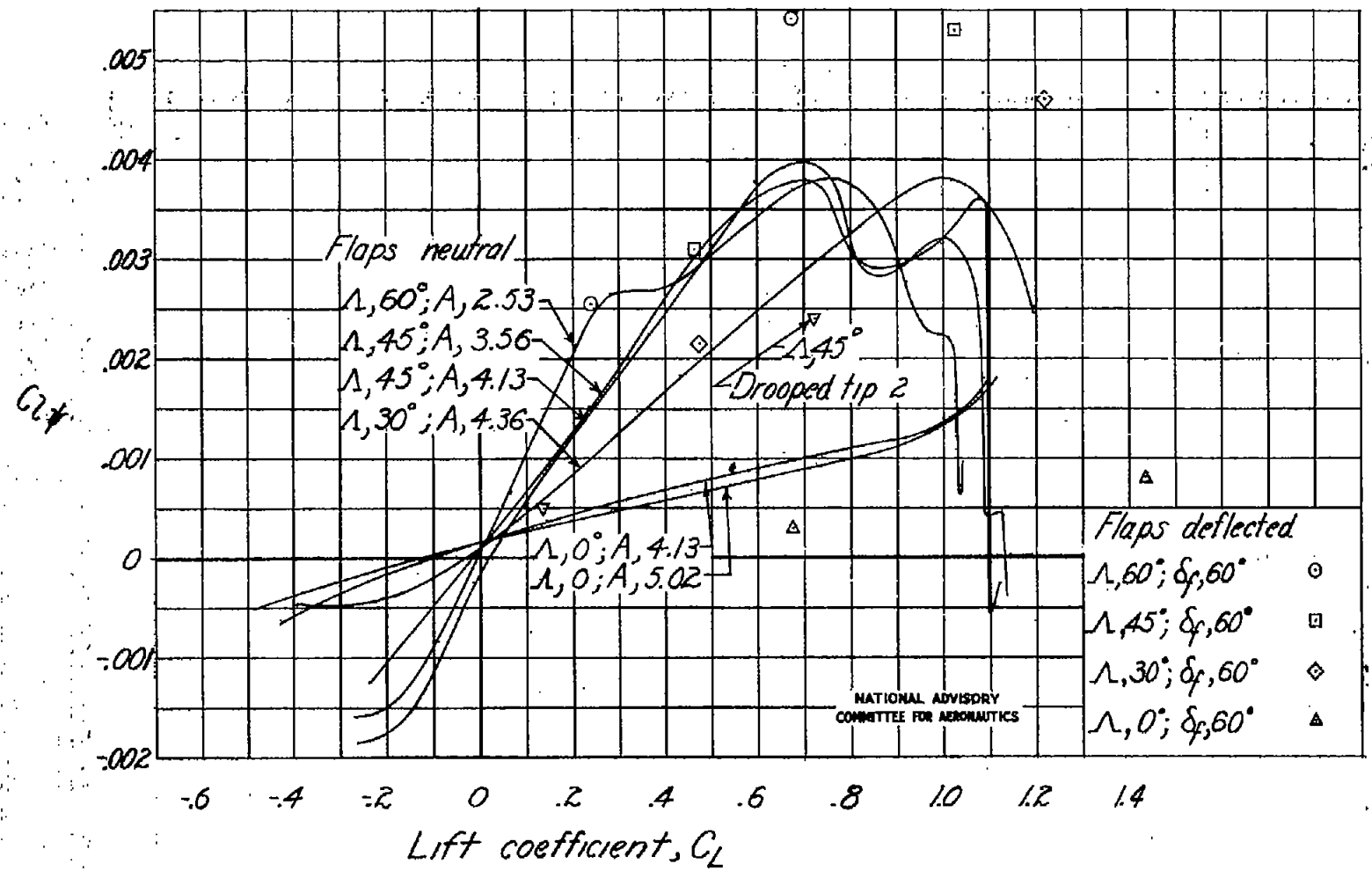

Figure 38.—Variation of C_{l_ψ} with lift coefficient for several angles of sweepback.

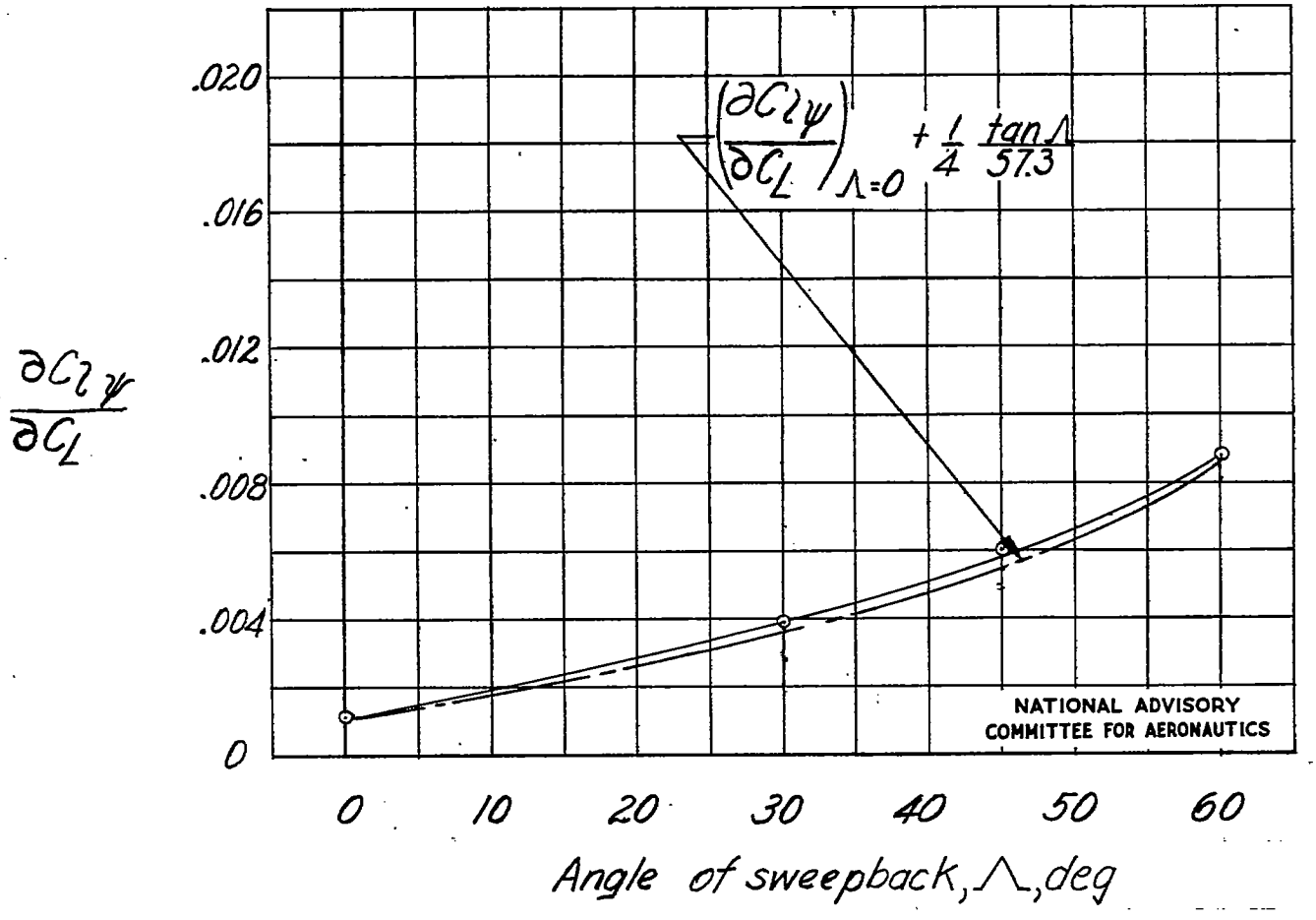

Figure 39.– Variation with sweepback of the estimated and experimental values of $\frac{\partial C_{l_\psi}}{\partial C_L}$.

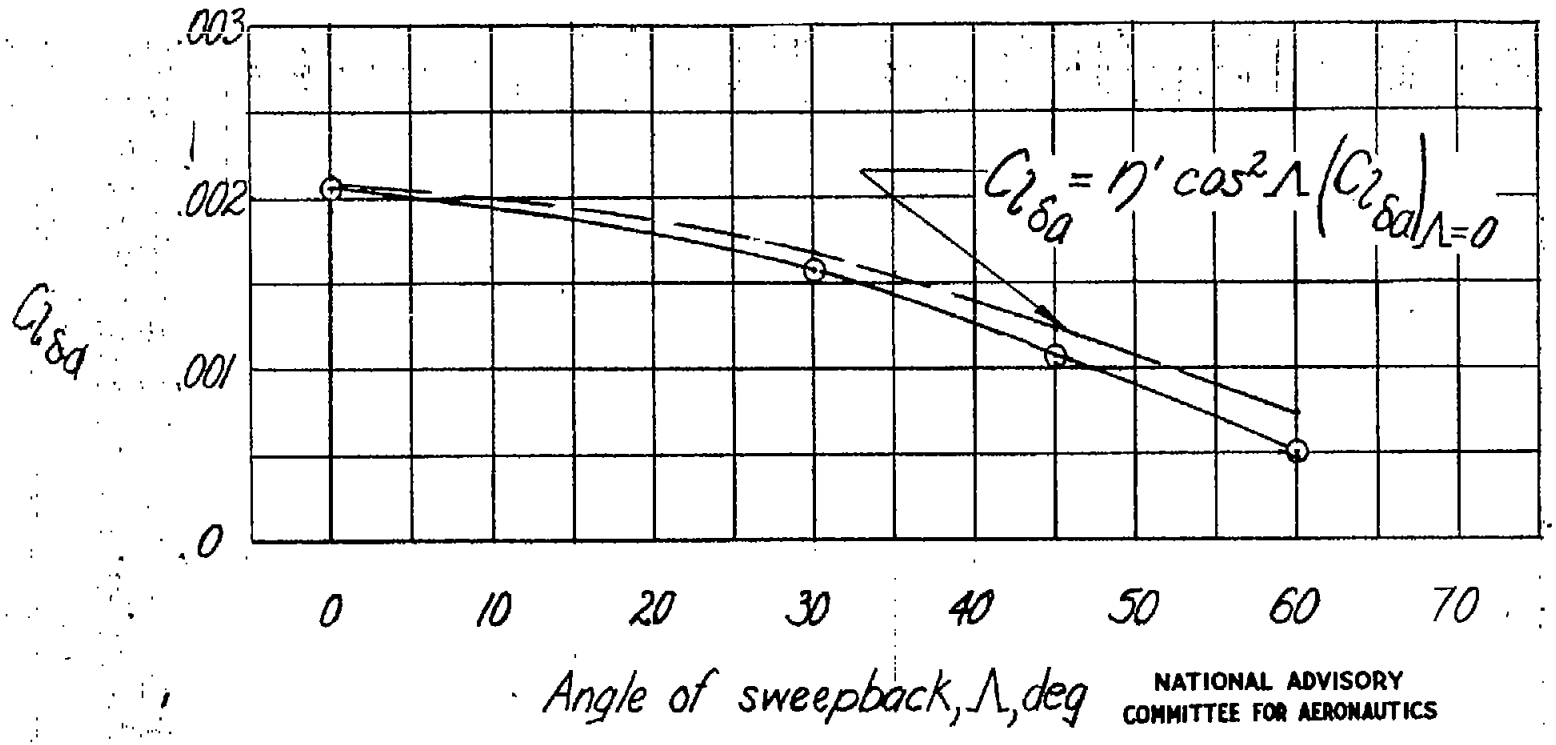

NATIONAL ADVISORY COMMITTEE FOR AERONAUTICS

Figure 40.- Variation with sweepback of the estimated and experimental values of $C_{l_{\delta a}}$ for $C_L = 0.2$.

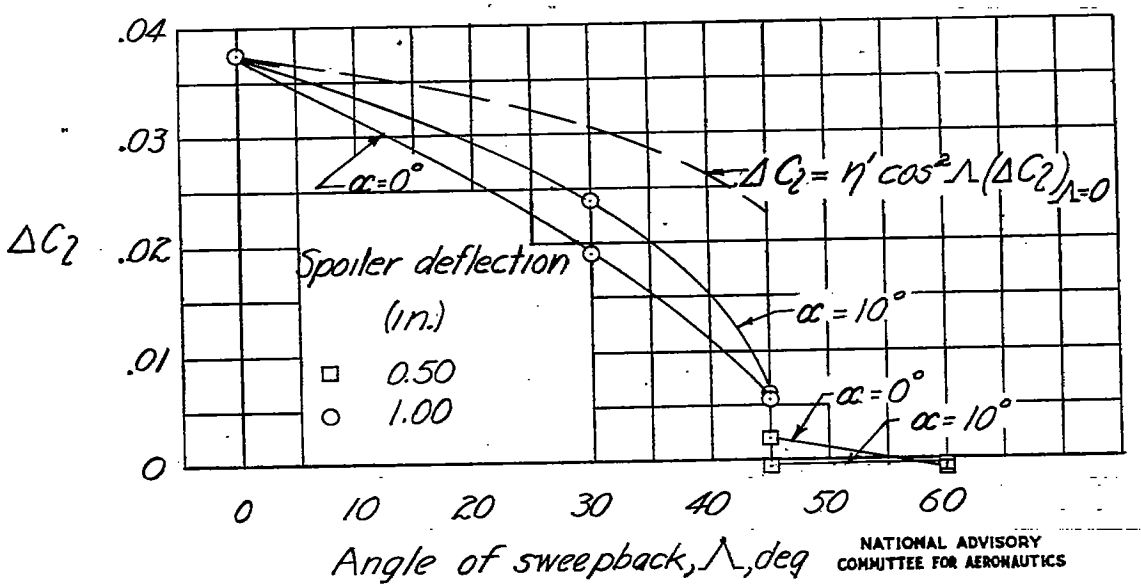

Figure 41.– Variation with sweepback of the estimated and experimental values of ΔC_l resulting from spoiler deflection.

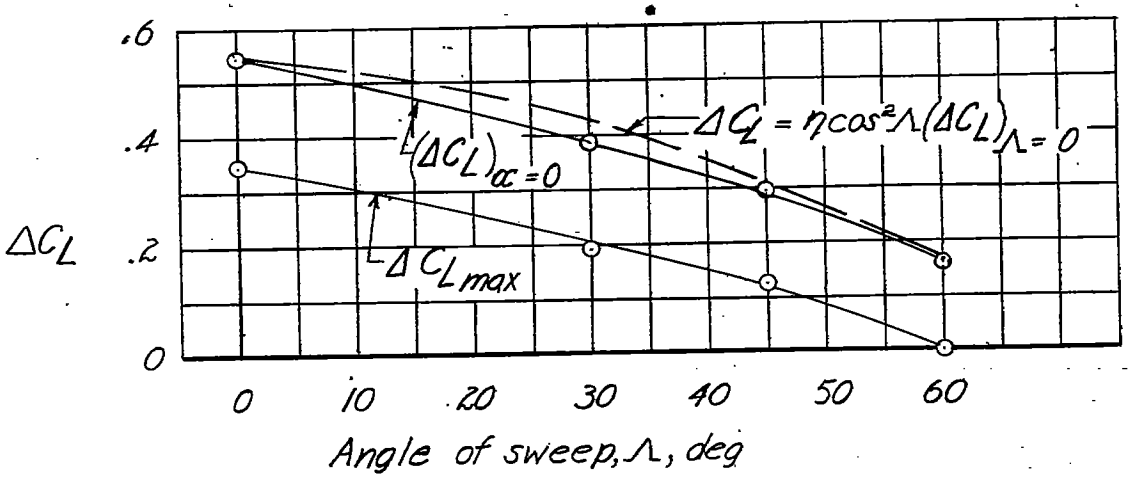

Figure 42.– Variation with sweepback of the estimated and experimental values of ΔC_L resulting from a split-flap deflection of 60°.

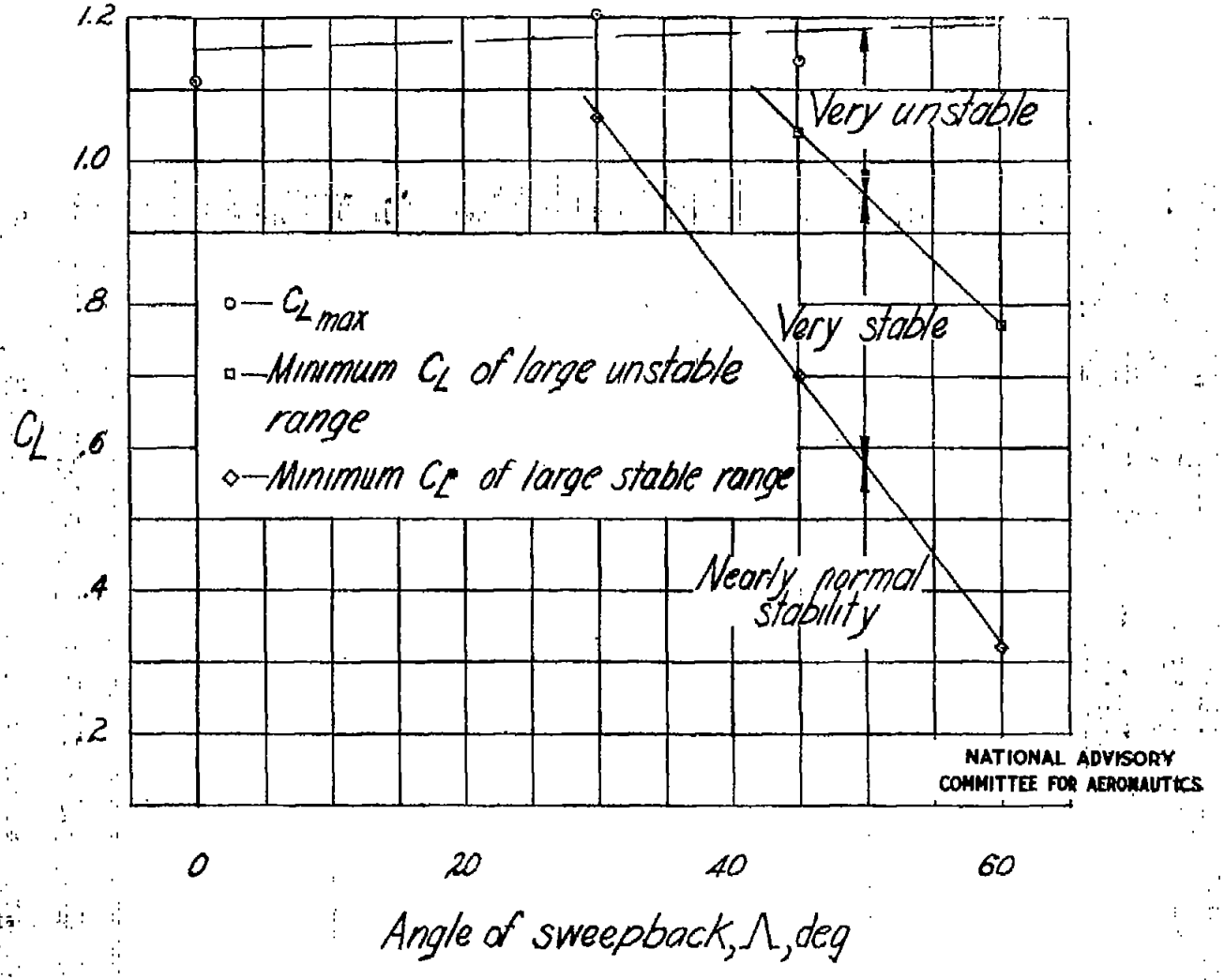

Figure 43.-Lift coefficients bounding the ranges of longitudinal stability for the various swept-back wings.